

The Paleocene-Eocene Thermal Maximum: A Perturbation of Carbon Cycle, Climate, and Biosphere with Implications for the Future

Francesca A. McInerney^{1,*} and Scott L. Wing²

¹Department of Earth and Planetary Sciences, Northwestern University, Evanston, Illinois 60208; email: cesca@earth.northwestern.edu

²Department of Paleobiology, National Museum of Natural History, Smithsonian Institution, Washington, DC 20013; email: wings@si.edu

Annu. Rev. Earth Planet. Sci. 2011. 39:489–516

First published online as a Review in Advance on March 1, 2011

The *Annual Review of Earth and Planetary Sciences* is online at earth.annualreviews.org

This article's doi:
10.1146/annurev-earth-040610-133431

Copyright © 2011 by Annual Reviews.
All rights reserved

0084-6597/11/0530-0489\$20.00

*Formerly Francesca A. Smith.

Keywords

PETM, global warming, paleoclimate, paleoecology, carbon cycle

Abstract

During the Paleocene-Eocene Thermal Maximum (PETM), ~56 Mya, thousands of petagrams of carbon were released into the ocean-atmosphere system with attendant changes in the carbon cycle, climate, ocean chemistry, and marine and continental ecosystems. The period of carbon release is thought to have lasted <20 ka, the duration of the whole event was ~200 ka, and the global temperature increase was 5–8°C. Terrestrial and marine organisms experienced large shifts in geographic ranges, rapid evolution, and changes in trophic ecology, but few groups suffered major extinctions with the exception of benthic foraminifera. The PETM provides valuable insights into the carbon cycle, climate system, and biotic responses to environmental change that are relevant to long-term future global changes.

INTRODUCTION AND BRIEF HISTORY OF STUDY

Almost 20 years ago Kennett & Stott (1991) published an account of rapid shifts in stable carbon and oxygen isotope ratios observed in species-specific foraminiferal carbonate from Ocean Drilling Program (ODP) Site 690B off the coast of Antarctica. Key features of the event were a rapid onset (which they estimated to be ~ 6 ka), a decline in oxygen isotope ratios (indicating warming of 3–4°C in surface water and $\sim 6^\circ\text{C}$ in deep water), a negative shift in the $\delta^{13}\text{C}$ of benthic ($\sim -2\text{‰}$) and planktic ($\sim -4\text{‰}$) forams, influx of a diverse surface water microfossil assemblage with subtropical affinities, an increase in kaolinite, and elimination or even reversal of depth gradients in both $\delta^{13}\text{C}$ and $\delta^{18}\text{O}$. All these changes were synchronous with an already-known extinction of benthic foraminifera (Thomas 1989).

Following the paper by Kennett and Stott on what has come to be known as the Paleocene-Eocene Thermal Maximum (PETM), Koch et al. (1992) measured the negative carbon isotopic excursion (CIE) in pedogenic carbonate and mammalian tooth enamel derived from continental rocks, and they recognized that the CIE coincided exactly with the largest mammalian faunal turnover of the Cenozoic. The paper by Koch et al. (1992) established the PETM as a global event that could be detected in the continental realm and showed how the CIE could be used to correlate marine and continental sections.

Recognition that the PETM was a global environmental shift associated with profound biological consequences attracted additional study, as did the problem of formalizing a Paleocene-Eocene boundary that could be used in both terrestrial and marine sections (e.g., Aubry 2000). By the end of the 1990s more than 50 papers had been published on the PETM, and the number has exceeded 400 as we write (**Figure 1, Supplemental Figures 1 and 2**). (To view the Supplemental figures, table, and accompanying references, follow the **Supplemental Materials link** from the Annual Reviews home page at <http://www.annualreviews.org>.) The literature on the PETM is now too extensive to review comprehensively, so we focus on changes in carbon cycle, paleoclimate, and biotas during the PETM.

AGE AND DURATION OF THE PALEOCENE-EOCENE THERMAL MAXIMUM

The Paleocene-Eocene boundary has been defined by the placement of a Global Boundary Stratotype Section and Point (GSSP) in the Dababiya Quarry section of Egypt and is most commonly recognized by the base of the CIE (Luterbacher et al. 2000). The age of the CIE onset has been estimated recently as 56.011–56.293 Ma, using radiometric dates of marine ash layers and orbital tuning of marine sediments (Westerhold et al. 2009). Zircons from the upper part of the CIE are estimated to be 56.09 ± 0.03 Ma, determined from chemical abrasion–thermal ionization mass spectrometry (Jaramillo et al. 2010). This is consistent with an onset at approximately 56.3 Ma. Prior to the establishment of the Paleocene-Eocene boundary, this same event was known as the Latest Paleocene Thermal Maximum (LPTM); following the boundary designation it was also termed the Initial Eocene Thermal Maximum (IETM). PETM is now widely used.

Two main approaches have been used to estimate the duration of the PETM: astronomical cyclostratigraphy and extraterrestrial ^3He fluxes. Orbital timescales suggest a total duration of 150–220 ka (Aziz et al. 2008; Röhl et al. 2003, 2007), whereas ^3He suggests 120–220 ka (Farley & Eltgroth 2003, Murphy et al. 2010). The onset of the CIE—that is, the time from the last samples with pre-CIE carbon isotope composition to the most depleted values—has been estimated to take place in less than 10 ka (Zachos et al. 2005), but the dissolution of uppermost Paleocene and lowermost Eocene carbonate associated with the CIE in many deep marine sections makes

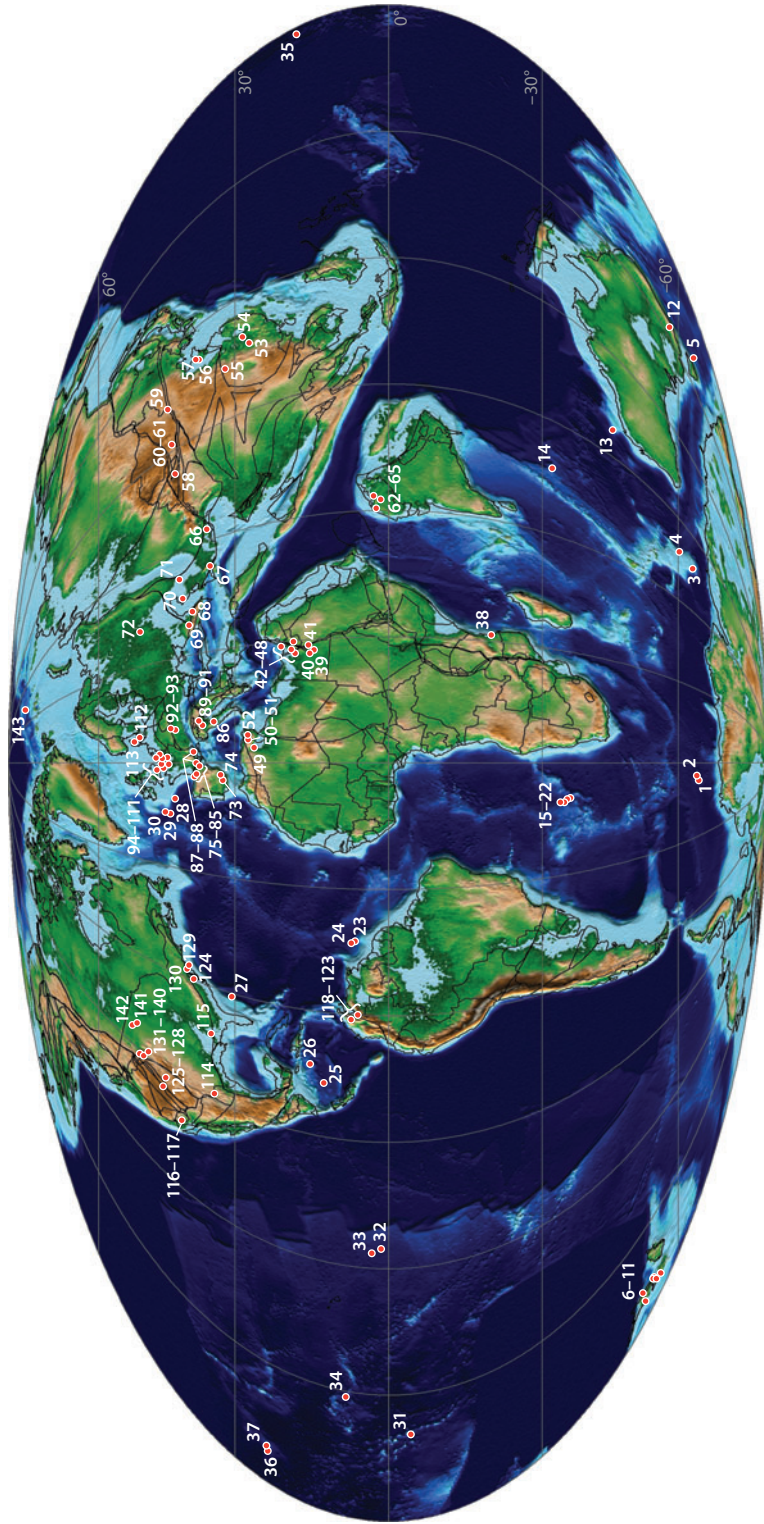


Figure 1

Global paleogeographic map for 56 Mya with marine and continental sites where the Paleocene-Eocene boundary interval has been studied. Background colors show relative elevation/bathymetric depth. Black lines indicate plate boundaries. Site numbers are keyed to **Supplemental Table 1**. Paleogeographic map and site positions by Scotese (2010). **Supplemental Figure 1** provides a high-resolution, editable version of this image. (To view the table and figure, follow the **Supplemental Materials** link from the Annual Reviews home page at <http://www.annualreviews.org>.)

it difficult to estimate the duration of the onset (Murphy et al. 2010). The onset of the CIE in continental sections, which are not affected by carbonate dissolution, occupies 4–7 m of section, equivalent to 8–23 ka based on calculated sedimentation rates (Aziz et al. 2008, Bowen et al. 2001, Magioncalda et al. 2004).

A central debate about the PETM timescale concerns the duration of the “recovery” from the CIE, during which carbon isotope composition returned almost to latest Paleocene values. Sediments of the recovery phase are roughly twice as thick as those from the “body” of the CIE (sensu Bowen et al. 2006) at ODP Site 690 on Maud Rise (Bains et al. 1999), but in many other marine and terrestrial records the recovery phase is shorter relative to the body of the excursion (Bowen et al. 2001, Giusberti et al. 2007, Zachos et al. 2005). In the most recent estimate of the duration of the CIE, based on ^3He calibration of depositional rates at ODP Site 1266 on Walvis Ridge, the body (or core) of the excursion is ~ 113 ka and the total recovery is ~ 83 ka, with ~ 33 ka in an early rapid phase (I) and ~ 50 ka in a subsequent gradual phase (II) (Murphy et al. 2010). The 1266 record, when calibrated to time using orbital cyclostratigraphy, has a body of ~ 59 ka and a total recovery interval of ~ 112 ka (Röhl et al. 2007). The difference in CIE time estimates for deep marine sediments probably arises from variation in sedimentation rates caused by carbonate dissolution at the onset of the CIE and enhanced carbonate deposition during the recovery phase (Kelly et al. 2005, 2010; Murphy et al. 2010). The one continental section that has been calibrated to time with orbital cycles (Polecat Bench, Wyoming) gives estimates of ~ 115 ka for the body and ~ 42 ka for what appears to be the rapid recovery (phase I) (Aziz et al. 2008). Because a long body and short recovery to the CIE are seen in ^3He -calibrated deep marine sections as well as shallow marine and continental sediments, they are likely better estimates of the true duration of the CIE and its phases.

ENVIRONMENTAL CHANGE DURING THE PALEOCENE-EOCENE THERMAL MAXIMUM

The PETM is defined by a global temperature rise that was initially inferred from a $> 1\%$ negative excursion in $\delta^{18}\text{O}$ of benthic foraminifera, indicating a deep-water temperature increase of $\sim 5^\circ\text{C}$ (Kennett & Stott 1991, Thomas & Shackleton 1996, Zachos et al. 2001). A similar magnitude of temperature increase has also been inferred from Mg/Ca ratios (Tripathi & Elderfield 2005, Zachos et al. 2003). Planktonic foraminiferal $\delta^{18}\text{O}$ and Mg/Ca ratios are also generally consistent with $\sim 5^\circ\text{C}$ of warming, though estimates reach up 8°C of warming at Wilson Lake, New Jersey (Zachos et al. 2006), and ODP Site 690, Maud Rise (Kennett & Stott 1991, Thomas et al. 2002). Although there is spatial variation in the amount of warming associated with the PETM, it is significant that temperature increase in the Arctic (Lomonosov Ridge) determined from biomarker paleothermometers (TEX $_{86}$ ' and GDGT) is ~ 5 – 8°C (Sluijs et al. 2006, Weijers et al. 2007). The absence of greater warming at polar latitudes during the PETM implies an absence of the ice-albedo feedback loop that would have generated more warming at high latitudes if sea or land ice had been present in the late Paleocene (Sluijs et al. 2006). A warming of ~ 5 – 7°C is also inferred from leaf margin analysis and oxygen isotope composition of fish scales, mammalian tooth enamel, and soil nodules in the fully continental Bighorn Basin, Wyoming (Bowen et al. 2001, Fricke & Wing 2004, Fricke et al. 1998, Koch et al. 2003, Wing et al. 2005).

Modeling of the PETM, as with equable climates of the early Cenozoic in general, has tended to produce temperatures in polar regions that are too cool (e.g., Huber et al. 2003, Shellito & Sloan 2006) even if the atmosphere is stipulated to have 16 times the preindustrial concentration of CO_2 in the atmosphere (Winguth et al. 2010). This persistent problem with modeling a PETM climate that has a low equator-to-pole temperature gradient and warm winters in mid-latitude continental

interiors may require consideration of the effect of methane or other trace greenhouse gases (Sloan et al. 1992) and clouds (Abbot & Tziperman 2009). Suggestions that tropical temperatures were $\gg 35^{\circ}\text{C}$ (Huber 2008), allowing for a steeper latitudinal gradient, are unlikely to be born out because terrestrial floras from the tropics become more rather than less diverse during the PETM (Jaramillo et al. 2006, 2010).

In addition to warming, there is widespread evidence for changes in runoff, often interpreted as indicating increased precipitation on the continents during the PETM. High abundance of kaolinite, a product of weathering in warm, wet climates, has been observed near the Paleocene-Eocene boundary in many marginal marine sections from Antarctica to eastern North America to North Africa and Pakistan (Bolle & Adatte 2001, Gibson et al. 2000, Robert & Kennett 1994). The influx of kaolinite, however, likely reflects erosion of previously formed clay, rather than weathering and erosion during the geologically brief PETM (Schmitz et al. 2001, Thiry & Dupuis 2000). The sharp increase in eutrophic dinoflagellate populations in coastal marine sections during the PETM has also been cited as evidence for enhanced terrestrial input (Crouch et al. 2001, 2003), which has in turn been equated with increased precipitation on land. In fact, the relationship between sediment production and precipitation is not positive and monotonic but rather unimodal, with the highest erosion and sediment loads occurring under highly seasonal precipitation of $\sim 300\text{--}600\text{ mm year}^{-1}$ (Cecil & DuLong 2003). Thus more terrestrial runoff in nearshore marine sediments is likely an indicator of higher seasonality or episodicity rather than greater precipitation. More episodic precipitation could explain enhanced export of terrestrial organic matter to the Arctic Ocean basin during the PETM (Boucein & Stein 2009, Pagani et al. 2006b) as well as higher iron content of marine carbonates in New Zealand (Villasante-Marcos et al. 2009).

Proxy data indicate higher variability of precipitation in a number of regions during the PETM. PETM sections in the Pyrenees of northern Spain (paleolatitude $\sim 35^{\circ}\text{N}$) include the distinctive and widespread Claret Conglomerate, a megafan deposit typical of areas with highly intermittent, violent rainfall (Schmitz & Pujalte 2007, Schmitz et al. 2001). Palynological assemblages from the same area indicate a loss of taxodiaceous conifers, which prefer wetter habitats (Schmitz et al. 2001). Recent evidence from silicon isotopes in paleosols from the Paris Basin, farther to the north, fails to indicate enhanced chemical weathering during the PETM, consistent with no increase in total precipitation (Rad et al. 2009). PETM marine deposits in Austria show a strong increase in siliciclastic deposition but remain dominated by smectite clays that indicate weathering under a seasonal subtropical climate; this has been interpreted as an increase in seasonality of precipitation leading to greater erosion and delivery of terrestrial material to the marine environment (Egger et al. 2005). In North America, paleosol horizons of PETM age in the Bighorn Basin of Wyoming (paleolatitude $\sim 49^{\circ}\text{N}$) indicate less chemical weathering (Kraus & Riggins 2007), and changes in ichnofossil assemblages are consistent with drier or better-drained soils (Smith et al. 2008a,b). In the same area, decrease in leaf size from latest Paleocene to early PETM floras reflects an increase in water stress (Wing et al. 2005, 2009). A more arid climate is indicated by paleosols from the southern Rocky Mountains (paleolatitude $\sim 44^{\circ}\text{N}$) during the PETM (Bowen & Bowen 2008).

Although general circulation models of PETM climate predict 10–20% higher precipitation in many continental areas (e.g., Huber & Sloan 1999, Winguth et al. 2010), available proxy data (mostly mid-latitude northern hemisphere) are more consistent with increased seasonality of precipitation, or more intense storms, rather than wetter climates. Higher precipitation is cited as a factor in increasing the rate of silicate weathering on the continents, which in turn has been proposed as a major cause of long-term drawdown of CO_2 from the atmosphere during recovery from the CIE (but see Bowen & Zachos 2010). We suggest that if higher precipitation were a major factor in higher rates of silicate weathering, it did not occur in the mid-latitude regions that are currently best sampled.

CARBON CYCLE CHANGES AT THE PALEOCENE-EOCENE THERMAL MAXIMUM

Two observations indicate a massive release of carbon at the PETM: the large, global negative CIE (Figure 2) and the extensive dissolution of deep-ocean carbonates. The negative shift in carbon isotope ($\delta^{13}\text{C}$) values shows that the carbon released was depleted in ^{13}C relative to the exogenic reservoir (ocean + atmosphere + biomass) and was likely organic carbon because organisms discriminate against ^{13}C during biosynthesis. The geologically rapid onset of the CIE (<20 ka) implicates the addition of ^{13}C -depleted (organic) carbon rather than a reduction in organic carbon burial (100 ka timescale; Kump & Arthur 1999). The sudden rise in the calcite compensation depth (CCD) (below which no calcite accumulates) at the onset of the CIE indicates that the ocean absorbed a large amount of CO_2 , reducing its pH and carbonate ion content [CO_3^{2-}] (Zachos et al. 2005). Although the large carbon release at the PETM is accepted, the source and mass of carbon are still actively debated. Five sources are being discussed:

- Methane clathrates: Methane clathrates are icy solids consisting of methane surrounded by water molecules. They are stable in deep-sea sediments, but they can be destabilized by increasing temperature caused by changes in ocean circulation (Dickens et al. 1995, 1997) or by decreasing pressure resulting from slope failure (Katz et al. 1999). This microbial methane has a $\delta^{13}\text{C}$ value of $\sim -60\text{‰}$ (Kvenvolden 1993).
- Wildfires: Burning of the extensive peat and coal deposited during the Paleocene ($\delta^{13}\text{C}$ of $\sim -22\text{‰}$) could have resulted from increasing atmospheric O_2 , dryer climates, and/or uplift of coal basins (Kurtz et al. 2003). However, no increase in combustion byproducts was observed in cores from either the Atlantic or Pacific (Moore & Kurtz 2008).
- Thermogenic methane: Injection of magma into organic-rich sediments would have caused the explosive release of thermogenic methane ($\delta^{13}\text{C}$ of $\sim -30\text{‰}$) from Cretaceous-Paleocene mudstones in the North Atlantic (Svensen et al. 2004, 2010; Westerhold et al. 2009).
- Drying epicontinental seas: Tectonically driven isolation of an epicontinental seaway would have led to rapid (<20 ka) desiccation and oxidation of organic matter ($\delta^{13}\text{C}$ of $\sim -22\text{‰}$) (Higgins & Schrag 2006). Though vast areas of central Asia were covered by shallow seaways in the Paleocene-Eocene, none are known to have dried up coincident with the PETM (Gavrilov et al. 2003).
- Permafrost: During the Paleogene, Antarctica did not support a large ice cap and may have stored vast quantities of carbon as permafrost and peat that could have been rapidly thawed and oxidized, releasing carbon ($\delta^{13}\text{C}$ of $\sim -30\text{‰}$) (DeConto et al. 2010).

How can these hypotheses be evaluated? Each source has a characteristic $\delta^{13}\text{C}$ value; thus the mass of carbon required to create the CIE can be calculated for each source (see sidebar, Mass Balance Calculations). These masses can be compared with the amount of carbon required to create the observed carbonate dissolution. In addition, these carbon releases must also be consistent with the observed warming given our understanding of the greenhouse effect. In spite of progress, the magnitude of the CIE, the amount of carbonate dissolution, and atmospheric $p\text{CO}_2$ levels remain difficult to quantify, as discussed below.

Mass Balance Accounting

Mass balance calculations require an estimate of the magnitude of the CIE in the exogenic carbon pool, but different archives vary widely. We compiled 165 carbon isotope records from the PETM, which show a mean CIE of -4.7 ± 1.5 (\pm standard deviation) for terrestrial records and -2.8 ± 1.3 for marine records (Table 1). Even within each realm archives differ. Comparison of median

MASS BALANCE CALCULATIONS

Steady-state isotopic mass balance is essentially instantaneous mixing. The final mass and isotopic ratio of carbon is the result of the initial mass and isotopic composition plus the mass and isotopic composition of added carbon. To calculate the mass of carbon added during the PETM, use the following equations:

$$(M_{\text{final}}) \times (\delta^{13}\text{C}_{\text{final}}) = (M_{\text{initial}}) \times (\delta^{13}\text{C}_{\text{initial}}) + (M_{\text{added}}) \times (\delta^{13}\text{C}_{\text{added}}). \quad (1)$$

M is mass of carbon and $\delta^{13}\text{C}$ is the carbon isotope ratio of each pool (initial, added, and final). Carbon isotope ratios are reported in delta notation as

$$\delta^{13}\text{C} = [(R_{\text{sample}}/R_{\text{standard}}) - 1] \text{ in per thousand or permil (‰) units,} \quad (2)$$

$$R = {}^{13}\text{C}/{}^{12}\text{C}, \quad (3)$$

$$M_{\text{final}} = M_{\text{initial}} + M_{\text{added}}, \quad (4)$$

$$\text{CIE} = \delta^{13}\text{C}_{\text{final}} - \delta^{13}\text{C}_{\text{initial}}. \quad (5)$$

By combining Equations 1, 4, and 5, the mass of carbon added can be calculated as

$$M_{\text{added}} = -\text{CIE} \times M_{\text{initial}} / (\delta^{13}\text{C}_{\text{final}} - \delta^{13}\text{C}_{\text{added}}). \quad (6)$$

In **Figure 3**, we calculate the mass added for each reservoir and CIE using estimates for the initial mass and carbon isotope ratio of the Paleocene surface reservoir as 50,000 Pg C (1 Pg = 1 Gt = 10^{15} g) (Archer 2007) and -2.5‰ (Killops & Killops 2005).

values shows that the smallest CIEs are in marine carbonates; intermediate CIEs are in marine and terrestrial organic matter; and the largest CIEs are in terrestrial plant lipids, mammalian tooth enamel, and pedogenic carbonate nodules (**Table 1, Figure 2**). A Kruskal-Wallis test rejects the null hypothesis that the CIEs for all groups are drawn from a single population ($p < 0.0001$); the marine and terrestrial records are also significantly different (Wilcoxon-Mann-Whitney test, $p < 0.0001$).

Which archive is most reliable? Marine carbonates are subject to severe dissolution during the PETM. Benthic foram and bulk carbonate $\delta^{13}\text{C}$ records clearly show greater dissolution and truncation of the CIE with increasing depth (McCarren et al. 2008, Zachos et al. 2005). The $\delta^{13}\text{C}$ of bulk organic matter in marine records is influenced by productivity and terrestrial input (Hilting et al. 2008); the $\delta^{13}\text{C}$ of bulk organic matter in the terrestrial realm is affected by soil respiration (Wynn 2007) and many other factors (e.g., Diefendorf et al. 2010, Smith et al. 2007). Soil carbonate $\delta^{13}\text{C}$ values vary with soil properties, atmospheric $p\text{CO}_2$, rate of carbon input, and rate of soil respiration (Bowen et al. 2004, Sheldon & Tabor 2009).

Terrestrial plants take up CO_2 directly from the atmosphere and therefore could provide the most reliable measure of the CIE. However, environmental factors such as water availability and intrinsic features such as plant functional type (e.g., conifer versus angiosperm) influence carbon isotope fractionation by C_3 plants (Diefendorf et al. 2010). Bowen et al. (2004) suggested increased water availability caused by an enhanced hydrologic cycle could have increased carbon isotope fractionation. Pagani et al. (2006b) argued that this was unlikely in the cool, wet Arctic,

Table 1 Summary of 165 records of the carbon isotopic excursion at the Paleocene-Eocene Thermal Maximum

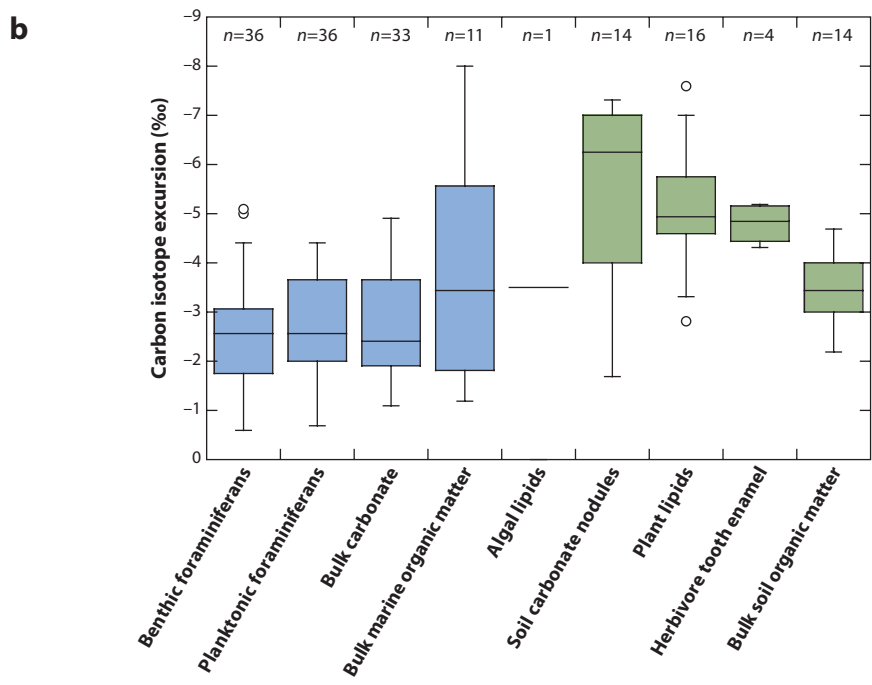
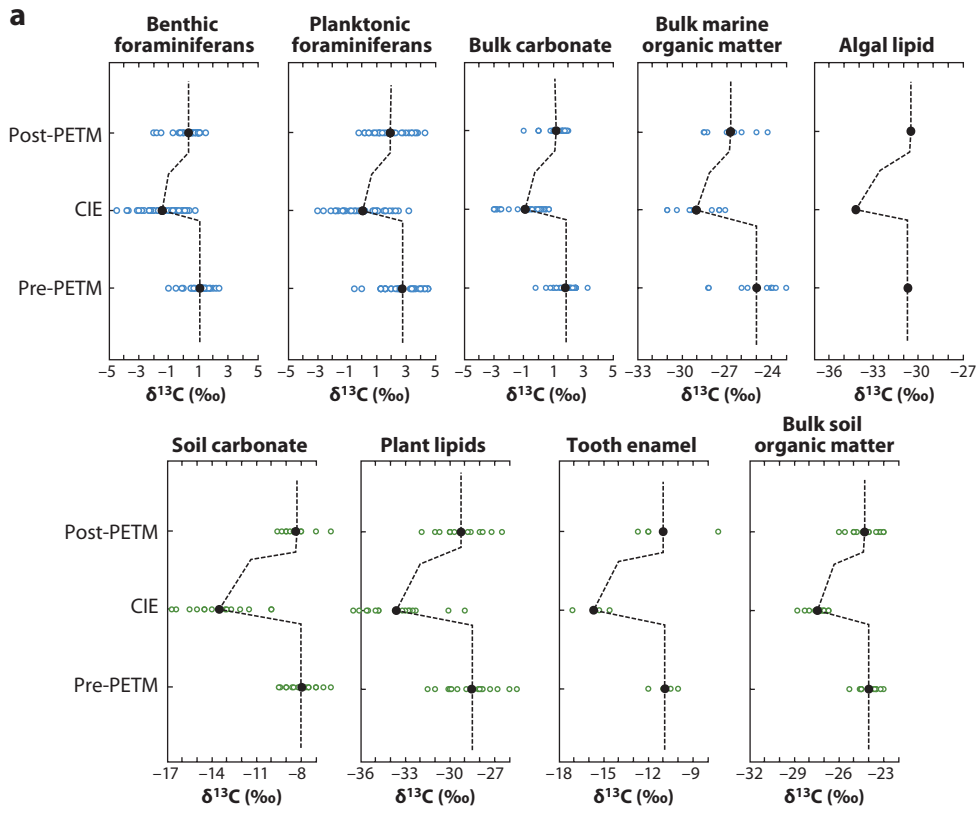
Archive	<i>n</i>	Minimum	Maximum	Average	Standard Deviation	Median
Benthic forams	36	−0.6	−5.1	−2.5	1.0	−2.6
Planktic forams	36	−0.7	−4.4	−2.7	1.0	−2.6
Bulk carbonate	33	−1.1	−4.9	−2.7	1.1	−2.4
Bulk marine organic matter	11	−1.2	−8.0	−4.1	2.2	−3.5
Algal lipid	1	−3.5	−3.5	−3.5	n/a	−3.5
Soil carbonate	14	−2.5	−7.3	−5.5	1.7	−6.3
Plant lipids	16	−2.8	−7.6	−5.1	1.3	−5.0
Bulk soil organic matter	14	−2.2	−4.6	−3.5	0.6	−3.5
Tooth enamel	4	−4.3	−5.2	−4.8	0.4	−4.9
All marine	117	−0.6	−8.0	−2.8	1.3	−2.6
All terrestrial	48	−2.2	−7.6	−4.7	1.5	−4.6

where leaf wax *n*-alkanes record a CIE of -5% . Smith et al. (2007) observed a negative CIE of -5% in leaf wax *n*-alkanes from the Bighorn Basin but pointed out that different chain-length *n*-alkanes recorded different CIEs, possibly indicating a shift from mixed conifer-angiosperm forest to purely angiosperm forest that amplified the CIE. Schouten et al. (2007) showed that plant functional type influences the magnitude of the CIE: Conifer terpenoids record a CIE of -3% , whereas angiosperm terpenoids record -6% . Diefendorf et al. (2010) quantified the isotopic effects of both precipitation and plant type. They concluded that the isotopic effect of a shift from conifers to angiosperms would have been largely counteracted by an overall decrease in plant fractionation caused by higher water use efficiency in response to higher water stress (Kraus & Riggins 2007, Wing et al. 2005).

Marine carbonates most likely underestimate the CIE; marine bulk organic matter and soil carbonates may overestimate it. McCarren et al. (2008) proposed the CIE was no smaller than -3.5% , as recorded in benthic forams from the shallowest, least truncated record on Walvis Ridge that best reflects the excursion in deep-ocean dissolved inorganic carbon, the largest reservoir of carbon in the exogenic pool. McCarren et al. (2008) also advocated that the CIE was no larger than -5% , the value from leaf-wax *n*-alkanes at the same site (Hasegawa et al. 2006). Diefendorf et al. (2010) produced a considered estimate of the atmospheric CIE (-4.6%) by accounting for the effects of both plant functional group and climate on fractionation. The releases associated with a CIE of -4.6% are 4,300 Pg C for methane clathrates, 10,000 Pg C for thermogenic methane or permafrost, and 15,400 Pg C for wildfires or epicontinental seas (Figure 3).

Figure 2

Measurements of the negative carbon isotopic excursion (CIE) at the Paleocene-Eocene Thermal Maximum (PETM) grouped by source material ($n = 165$; see **Supplemental Material** for references). (a) Each record is characterized by the pre-PETM mean, the most negative data point within the CIE (or average for that sample level), and the post-PETM mean (blue circles represent marine records; green circles represent terrestrial records). The dashed lines are the generalized shape of the CIE connecting the means of the plotted values (black circles). All x-axes represent 10% . (b) The CIE for each archive is shown in the box-and-whisker plots. The horizontal line represents the median; the box identifies the upper and lower quartile and contains 50% of the data; the whiskers identify the range; open circles are outliers.



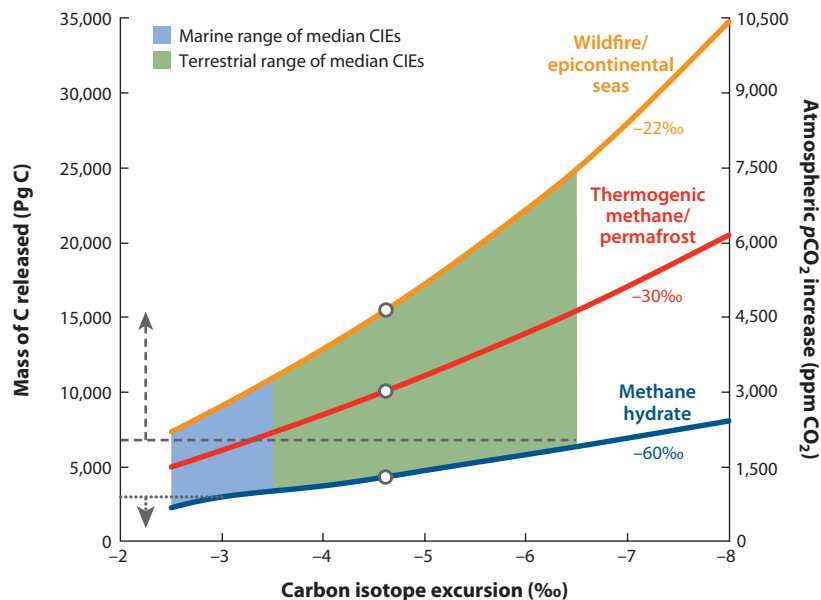


Figure 3

Mass balance estimates (see sidebar, Mass Balance Calculations) of mass of carbon released from different sources over a range of absolute values for the carbon isotopic excursion (CIE). Carbon sources: terrestrial wildfires or oxidation of organic matter from epicontinental seas ($\delta^{13}\text{C} = -22$); thermogenic methane or thawed permafrost ($\delta^{13}\text{C} = -30$); methane hydrate ($\delta^{13}\text{C} = -60$). Area shaded blue indicates marine range of median CIEs. Area shaded green represents terrestrial ranges for median CIEs (Table 1). Open circles represent masses for CIE of -4.6‰ (Diefendorf et al. 2010). Dashed horizontal line indicates minimum carbon release of 6,800 Pg C from modeling of carbonate dissolution allowing for variable bioturbation (Panchuk et al. 2008). Dotted horizontal line represents maximum mass initial release of 3,000 Pg C estimated by modeling carbonate dissolution while allowing for changes in ocean circulation (Zeebe et al. 2009). Second y-axis converts the mass of carbon released to an increase in atmospheric CO_2 (1 Pg C = 0.3 ppm CO_2) derived from the Grid ENabled Integrated Earth system (GENIE) model for late Paleocene ocean alkalinity, dissolved inorganic carbon, and seafloor carbonate content (Panchuk et al. 2008).

Carbonate Dissolution Accounting

The carbon release can be constrained by the CO_2 required to cause the observed dissolution of marine carbonates. On the basis of a depth transect in the Southeast Atlantic at Walvis Ridge, Zachos et al. (2005) estimated that the CCD shoaled by >2 km and that 4,500 Pg C would be required to cause similar CCD shoaling globally. However, the CCD rose by only ~ 500 m in the Pacific (Colosimo et al. 2006).

Two recent studies take a spatially explicit approach to modeling the observed pattern of dissolution in different ocean basins. Panchuk et al. (2008) coupled a three-dimensional ocean and atmosphere circulation model (GENIE-1) to models of the marine carbon cycle and seafloor sedimentation. Importantly, their sediment model allowed for predictions of wt% CaCO_3 with variable bioturbation, which mixes layers of sediment, increasing buffering capacity per unit area of seafloor. Bioturbation appears to have been reduced in the Atlantic during the PETM (Dickens 2000, Ridgwell 2007). Panchuk et al. (2008) estimated a minimum release of 6,800 Pg C over 10 ka, assuming no bioturbation in the Atlantic and deep Pacific during the PETM.

Zeebe et al. (2009) used the long-term ocean-atmosphere-sediment carbon cycle reservoir model (LOSCAR). To explain the observed difference in magnitude of shoaling in different ocean basins, they assumed an increase in formation of North Pacific deep water (NPDW) led to more corrosive deep waters in the Atlantic and that a portion of carbon was directly injected into the deep Atlantic. A maximum initial injection of 3,000 Pg C over 5 ka explains the observed dissolution in both the Pacific and the Atlantic. To model the shape of the excursion, they followed the initial pulse with a sustained release of 1,480 Pg C over 50 ka.

Although these studies differ in many details, three main factors cause the different estimates of the size of the carbon pulse. First, Panchuk et al. (2008) calculated circulation in the atmosphere and ocean using physical principles, whereas Zeebe et al. (2009) prescribed circulation. Second, Panchuk et al. (2008) calculated the pre-PETM CCD in their model and obtained a deeper Pacific CCD than did Zeebe et al. (2009), who estimated their pre-PETM CCD from sediment cores. The deeper pre-PETM Pacific CCD obtained by Panchuk et al. requires more carbon to reach the observed PETM CCD level. Third, Panchuk et al. (2008) explored the role of bioturbation, whereas Zeebe et al. (2009) examined the role of increased NPDW formation in the differential dissolution in the Pacific and the Atlantic. Discerning which approach most accurately reconstructs carbonate dissolution at the PETM will require a better understanding of the relative importance of bioturbation versus NPDW formation in modulating deep-ocean acidification.

Climate Sensitivity Accounting

Climate sensitivity refers to the temperature increase associated with a doubling of atmospheric CO₂ and all the associated physical, chemical, and biological climate feedbacks. Estimates range from 1.5°C to 4.5°C per doubling (IPCC 2007), which would imply between 1.1 and 3.3 doublings of *p*CO₂ to cause 5°C of PETM warming. Proxy estimates for Paleocene *p*CO₂ are scarce and range widely, from 200 ppm to 2,800 ppm (Breecker et al. 2010, Hilting et al. 2008, Pearson & Palmer 2000, Royer 2006, Royer et al. 2001). Assuming pre-PETM *p*CO₂ values of 600–2,800 ppm, 1.1 to 3.3 doublings would equate to an increase of 700–25,000 ppm CO₂ or the addition of 2,300–83,000 Pg C (see **Figure 3**; see also Pagani et al. 2006a).

Causes of the Paleocene-Eocene Thermal Maximum

Ideally, carbonate dissolution and climate sensitivity constraints would converge on a carbon release that, when compared with mass balance calculations based on the CIE, would identify the likely source(s) of carbon. Modeling of carbonate dissolution yields nonoverlapping solutions of less than of 3,000 Pg C initially (Zeebe et al. 2009) or more than 6,800 Pg C (Panchuk et al. 2008). Consideration of climate sensitivity leads to an estimate of >5,400 Pg C (Pagani et al. 2006b). Our current best estimate for the CIE of –4.6‰ (Diefendorf et al. 2010) yields a carbon release of 4,300 Pg C for methane clathrates and >10,000 Pg C for all the other sources. Thus, modeling of carbonate dissolution by Panchuk et al. (2008) and climate sensitivity (Pagani et al. 2006a) indicates that methane clathrates could not have been the source, whereas the carbonate modeling of Zeebe et al. (2009) suggests methane clathrates were the only viable source. Zeebe et al. (2009) recognize that their modeled carbon release would be insufficient to cause the full warming and argue for other unknown climate feedbacks or forcings as the cause of the remainder of the warming.

Atmospheric CO₂ concentrations during the latest Paleocene are critical to estimating the amount of carbon required to generate PETM warming. Pagani et al. (2006b) assumed a minimum *p*CO₂ of 600 ppm in the Paleocene because high *p*CO₂ is required to simulate warm poles in

GCMs. Many proxies for $p\text{CO}_2$, however, suggest values of ~ 400 ppm (Breecker et al. 2010, Hilting et al. 2008, Pearson & Palmer 2000, Royer 2006, Royer et al. 2001). If these proxies are correct, two doublings (to 1,600 ppm) would yield the addition of 1,200 ppm CO_2 or 4,000 Pg C and a warming of 6°C , assuming a standard climate sensitivity of 3°C per doubling (**Figure 3**). Methane clathrates would then be a viable source from a mass balance perspective. However, a strong argument against methane clathrates is that the mass of carbon held in Paleocene clathrates was likely too small ($\sim 1,000$ Pg C) to produce the observed CIE (Buffett & Archer 2004). Mass balance estimates of the carbon required from methane clathrates have increased from 1,200 Pg C (Dickens et al. 1997) to 4,300 Pg C as the estimated CIE has increased from -2.5‰ (Dickens et al. 1997) to -4.6‰ (Diefendorf et al. 2010). If the estimate of Buffett & Archer (2004) is correct, a different source or combination of sources would be required.

Early work described the CIE as a single release with an asymptotic return to more positive $\delta^{13}\text{C}$ values (Dickens et al. 1997), but recent marine and continental records show a ~ 100 -ka interval during which isotope values are low but stable, referred to as the body of the CIE (Bowen et al. 2006, Sluijs et al. 2007a) or the core (Murphy et al. 2010). The body of the CIE could indicate an alternate stable state of the carbon cycle (Bowen et al. 2006) or the continued release of light carbon (Zeebe et al. 2009) from one or more sources. Evidence is mounting for a $\sim 4^\circ\text{C}$ warming prior to the onset of the CIE, which also suggests multiple releases and possibly multiple sources of carbon (Secord et al. 2010, Sluijs et al. 2006).

Thermogenic methane and Antarctic permafrost/peat have intermediate isotopic signatures and require 10,000 Pg C for a CIE of -4.6‰ . This mass could explain both the observed warming and the modeled carbonate dissolution according to Panchuk et al. (2008). The organic rich rocks in the North Atlantic Volcanic Province, the source of thermogenic methane, would have held vast amounts of carbon (Svensen et al. 2004). Sufficiently large carbon stocks (potentially $> 10,000$ Pg C) also could have been stored on Antarctica because of greater land area and longer accumulation time in the Paleocene (DeConto et al. 2010). Both sources are capable of multiple and prolonged releases of carbon. Although debate is ongoing, the Antarctic permafrost/peat hypothesis has the power to explain not only the PETM but also the magnitude and pacing of the subsequent hyperthermals that occur in the following ~ 3 Ma (ETM2 and ETM3). These warm periods coincide with high eccentricity and obliquity capable of melting Antarctic permafrost (DeConto et al. 2010). In addition, the recharge of the Antarctic soil carbon reservoir would have helped the recovery phase and prepared the system for the next release. Each subsequent release would be expected to be smaller, as observed, because of the overall depleted carbon stocks (DeConto et al. 2010). Therefore, Antarctic peat and permafrost present intriguing potential sources for the carbon released at the PETM and subsequent hyperthermals.

Natural Carbon Sequestration: The Recovery Phase

Following the body of the CIE, which lasted ~ 113 ka, carbon isotope values and temperatures returned to near pre-PETM values over ~ 83 ka (Murphy et al. 2010). This recovery phase represents natural carbon sequestration and negative feedbacks that curtailed the CO_2 -induced warming. Three mechanisms have been proposed for the drawdown of CO_2 : increased C storage in the terrestrial biosphere (Beerling 2000, Bowen & Zachos 2010), increased marine export production (Bains et al. 2000, but see Torfstein et al. 2010), and enhanced silicate weathering on land with increased preservation of carbonates in the ocean (Kelly et al. 2005, 2010; Ravizza et al. 2001; Torfstein et al. 2010). Bowen & Zachos (2010) point out that the initial carbon isotope recovery is quite rapid, occurring over ~ 30 ka, and therefore likely required a process that preferentially sequestered ^{13}C -depleted carbon, such as the burial of organic matter in soils and peats.

BIOTIC EFFECTS OF THE PALEOCENE-EOCENE THERMAL MAXIMUM

Marine Ecosystems

The effects of the PETM on marine ecosystems have been documented in more than 50 cores and outcrop sections from near the North Pole through the tropics to offshore Antarctica, from open oceans to shallow coastal seas, and from almost every major ocean basin and continental margin (Figure 2). In spite of the geographic extent and environmental spread of marine records, no macroinvertebrate fossil assemblages have been described from the PETM (Ivany & Sessa 2010), so PETM effects on marine ecosystems are seen entirely through microfossils.

Even before the Paleocene–Eocene transition was recognized as a major perturbation of climate and carbon cycle it was known as the interval of the largest benthic foraminiferal extinction in the past 90 Ma, removing 30–50% of benthic foraminiferal diversity (Thomas 1989, 1998, 2003, 2007; Tjalsma & Lohmann 1983). This is often referred to as the benthic foram extinction or benthic extinction event, and it marks the rapid transition from the Cretaceous–Paleocene fauna to the Eocene fauna—one of only three major shifts in benthic foram faunas since the mid-Mesozoic (Thomas 1998, 2007).

The extinction, which begins near the onset of the CIE, was most severe at middle bathyal and greater depths, but shallower faunas also underwent rapid changes in composition as well as some extinction (Alegret et al. 2009a,b; Aref & Youssef 2004; Thomas 1998). Throughout the CIE, benthic foram faunas at all depths have low diversity and high dominance, and they are composed largely of small, thin-walled or agglutinated (noncalcareous) species (Thomas 2007). Detailed studies of the benthic foram extinction at Alamedilla and Zumaia in Spain show that the extinction was rapid but not ecologically instantaneous (Alegret et al. 2009a,b).

The benthic foram extinction has been attributed to increased corrosivity of deep waters, lower oxygen levels, changes in food supply, and higher temperatures (Thomas 2003, 2007). There is evidence for change in all these environmental variables in at least some parts of the ocean, but with the exception of temperature, none of them affected the sea floor globally, favoring the idea that the temperature increase of 4–5°C was the ultimate driver of extinction (Alegret et al. 2009a,b; Sluijs et al. 2007b; Thomas 2007). How warming would have driven extinction is less clear: Thomas (2007) proposed that higher temperatures increased the metabolic rates of benthic forams, the microbes they consumed, and their metazoan predators, with cascading effects on species at each trophic level.

In contrast to the marked extinction of benthic foraminifera, other groups of benthic and planktic microfossils show little or no extinction at the PETM. Ostracodes are the only other group of deep benthic organisms with detailed records across the PETM, and their response ranges from decreased diversity and abundance (Steineck & Thomas 1996), to little change in diversity or relative abundance distribution (Webb et al. 2009), to rapid changes in ostracode species composition (Morsi et al. 2011, Speijer & Morsi 2002).

Planktic forams shifted geographic ranges during the PETM. The tropical genus *Morozovella* occurred at high latitude sites just before and during the early part of the PETM (Thomas & Shackleton 1996), and an increase in warm climate forams is seen in many middle and lower latitude sites either just before or at the onset of the PETM (Arenillas et al. 1999, Berggren & Ouda 2003, Lu & Keller 1995, Pardo et al. 1999).

Forams also exhibit rapid evolutionary change in form during the PETM. In the Pacific, planktic forams increased in size while benthic forams decreased in size (Kaiho et al. 1996, Petrizzo 2007). Body-size increase in planktic forams may reflect the success of larger individuals with

greater capacity for photosymbionts in the oligotrophic surface waters created by thermal stratification (Kaiho et al. 1996). Benthic dwarfing may have been mediated by the effect of temperature on bottom-water oxygenation, with smaller forams favored in less oxic conditions (Kaiho et al. 2006), though higher temperatures may also have increased metabolic rates, causing food to become limiting (Alegret et al. 2010). Rapid diversification and morphological evolution of planktic forams have also been observed in the Pacific, with PETM “excursion taxa” having distinctive morphology that evolved in <10 ka and persisted only through the PETM (Kelly et al. 1996, 1998). Detailed morphometric and stable isotopic analyses suggest that ancestral populations temporarily collapsed. Furthermore, in some lineages, the descendants may have originated suddenly from peripherally isolated populations, whereas other lineages may have undergone sympatric speciation (Kelly et al. 1998). As with increasing size, morphological specializations of the tests may be related to supporting photosymbionts.


Larger forams were a major reef-forming group in shallow tropical seas during the late Paleocene (Hottinger 1998, Scheibner & Speijer 2008, Scheibner et al. 2005), perhaps because their algal symbioses are more resistant to high temperatures (Hallock 2000). With the PETM there was a major turnover in larger foram community composition (Pujalte et al. 2009): Species thought to be the most specialized for oligotrophic conditions were eliminated (Scheibner et al. 2005). This is consistent with a transient increase in productivity in shallow parts of Tethys (Bolle & Adatte 2001, Crouch et al. 2001, Egger et al. 2005, Ravizza et al. 2001, Scheibner & Speijer 2008, Speijer & Morsi 2002).

Nannofossils, the calcareous platelets of unicellular marine algae (e.g., Coccolithophorida), also show significant but geographically heterogeneous changes during the PETM (Agnini et al. 2007; Bown & Pearson 2009; Bralower 2002; Gibbs et al. 2006b; Jiang & Wise 2007; Monechi et al. 2000; Raffi et al. 2005, 2009). The main factors influencing nannoplankton were probably temperature and nutrient availability (Gibbs et al. 2010). Nannofossils favoring oligotrophic conditions became more abundant at open ocean sites (Bralower 2002, Gibbs et al. 2006b, Tremolada & Bralower 2004), but eutrophic nannofossils increased in some marginal seas (Agnini et al. 2007, Angori et al. 2007, Gibbs et al. 2006b). Off Antarctica, warm-water nannofossils replaced cold-water taxa (Angori et al. 2007), and at lower latitudes cool-water taxa were eliminated (Bown & Pearson 2009, Mutterlose et al. 2007). Rates of species extinction and origination were extremely high globally among nannofossils, especially near the onset of the CIE, with the PETM exhibiting the highest rates of turnover for the Cenozoic (Gibbs et al. 2006a).

One of the most salient events among marine plankton during the PETM is the large increase in abundance and geographic range of the heterotrophic dinoflagellate *Apectodinium* (Bujak & Brinkhuis 1998; Crouch et al. 2001, 2003; Sluijs et al. 2005, 2006; for a review see Sluijs et al. 2007a). This lineage, which had been largely restricted to low latitudes in the late Paleocene, expanded to polar latitudes in both hemispheres during the PETM, attaining abundances of >40% of dinocysts in many samples. *Apectodinium* was able to spread to higher latitudes because of higher temperature, but the abundance of this heterotroph may be related to higher nutrient levels near the continents (Sluijs et al. 2007b).

Terrestrial Ecosystems

PETM sections containing terrestrial fossils and biomarkers have been described from the Arctic Ocean, North America, northern South America, western Europe, central and south Asia, east Asia, and New Zealand (**Figure 1, Supplemental Table 1**). North America has the greatest number and geographic extent of continental and continental margin PETM sites, including sites from the Arctic to the southern shore of the continent, and from intramontane and foreland basins in the

 Supplemental Material

Rocky Mountains to marginal marine settings of the Gulf and Atlantic Coastal Plains. Given the heterogeneity of terrestrial climates and biotas, it is not surprising that faunal and floral responses to the PETM differ by continent and region.

For more than a century it has been recognized that a burst of mammalian first appearances occurs at the base of the Eocene, including the earliest even-toed ungulates (Artiodactyla), odd-toed ungulates (Perissodactyla), primates (not including Plesiadapiformes), and Hyaenodontidae (Gingerich 1989, 2003, 2006; Hooker 1998; Rose 1981 and references therein). Koch et al. (1992, 1995) showed that the first appearances of these taxa in the northern Rocky Mountains coincided closely with the onset of the CIE and suggested that the new mammals dispersed to North America across high latitude land bridges while the climate was warm. This faunal turnover is sometimes referred to as the mammalian dispersal event and is seen in European as well as North American faunas (Hooker 1998).

Fine stratigraphic resolution of mammalian faunal change and direct correlation with the CIE have been achieved at Polecat Bench in the Bighorn Basin (Bowen et al. 2001; Gingerich 1989, 2001). The body of the CIE is 40–45 m thick in this section (Bains et al. 2003, Bowen et al. 2001, Magioncalda et al. 2004). The onset of the CIE here is in rocks producing Clarkforkian (late Paleocene) mammals, but within a few meters of section, just below the level where the isotopic composition of pedogenic carbonate nodules reaches its nadir, the mammal *Meniscotherium* and a member of the Perissodactyla appear in the record (Gingerich 2003, 2006). A few meters higher, in the lowest part of the body of the CIE, the rest of the mammalian immigrant taxa appear (Wa0 zone of Gingerich 2003 and Gingerich 2006, earliest Eocene). The Wa0 immigrants are abundant from their first appearances, retain their abundance for millions of years subsequent to the PETM, and cause a major shift in mammalian trophic adaptations and body-size distributions (Clyde & Gingerich 1998). The Wa0 fauna has an unusually high abundance of digging mammals—taeniodonts and palaeonodonts (Gingerich 1989).

The Polecat Bench section has been calibrated to time by correlating the shape of the CIE measured in paleosol carbonate nodules with the orbitally calibrated CIE in bulk carbonate from ODP Site 690 (Bains et al. 2003), by interpolating stratigraphic thickness between magnetochron boundaries (Secord et al. 2006), and by cyclostratigraphy using paleosol color (Aziz et al. 2008). These methods give sedimentation rates of 0.3–0.5 m ka⁻¹, indicating the onset of the CIE was 10–15 ka before the first mammalian immigrants (including *Meniscotherium*) and 18–27 ka before the lowest Wa0 fauna.

The source of the PETM mammalian immigrants to North America is not fully known, but Bowen et al. (2002) showed that the extinct family Hyaenodontidae occurs just below the base of the CIE in the Hengyang Basin of south China, indicating that this group moved from Asia to North America. Although not conclusive, mammalian faunas from Inner Mongolia are consistent with the simultaneous appearance of the Primates, Artiodactyla, and Perissodactyla in Asia and North America (Bowen et al. 2005). The continent of origin for these three orders is still unknown (Clyde et al. 2003). Studies by Smith et al. (2006) and Beard (2008) purport to fix the direction of range expansion in primates by correlating their earliest occurrences in Europe, North America, and Asia using the shape of the CIE, but this approach is hampered by differences in the shape of the CIE in each area that are caused by local changes in depositional rate and by stratigraphic uncertainty in the level of first occurrence of primates resulting from the small number of specimens.

Mammals were not the only vertebrate group that underwent major compositional change at the PETM. At least seven species of lizards described from the PETM in Wyoming were recent immigrants to the region, and six of the seven belong to groups whose living members are found only in frost-free areas of the Americas (Smith 2009). With one possible exception, lizard dispersal during the PETM was intracontinental rather than intercontinental. Turtles also have several first

occurrences during or immediately after the PETM in Wyoming, including lineages with both Asian and American distributions (Bourque et al. 2008, Holroyd et al. 2001).

In addition to the dispersal event, mammalian faunas of the Wa0 zone are distinctive because of their small body size, with 11 lineages, both immigrants and natives, known from individuals about half the body weight of their pre- and/or post-PETM relatives (Chester et al. 2010; Gingerich 1989, 2006; Strait 2001). In the southeastern Bighorn Basin, dense sampling of perissodactyls shows that body size decreased dramatically from their first occurrence near the onset of the CIE to the middle of the body of the CIE, which in marine records is the warmest part of the PETM (Secord et al. 2008). The rapid “dwarfing” could be related to increasing temperature and/or to a decrease in the protein content of plants as a consequence of the reduced production of the photosynthetic protein Rubisco under high atmospheric CO₂ levels (Gingerich 2006). However, the latter hypothesis does not appear to account for the dwarfing of omnivorous or faunivorous mammals, unless change in climate and atmospheric composition also lowered net primary productivity (Chester et al. 2010), which is directly correlated with mammalian body size across modern gradients (Yom-Tov & Geffen 2006). Soil faunas also dwarfed during the CIE, perhaps because of increasing temperature and/or declining productivity (Smith et al. 2009).

Early paleobotanical studies of the PETM found little change across the Paleocene-Eocene transition (Wing 1998, Wing & Harrington 2001), but they lacked samples from the PETM. Once megafloras were found within the CIE they proved to be radically different in composition from those immediately before and after (Wing et al. 2005). Pre- and post-PETM megafloras are a mix of deciduous and evergreen broad-leaved lineages (e.g., birches, katsura, walnuts, elms, and laurels) as well as conifers in the bald cypress family (Wing 1998, Wing et al. 1995). PETM megafloras lack conifers and are dominated both in diversity and abundance by the bean family, important in dry tropical and subtropical areas today (**Figure 4**; Smith et al. 2007; Wing et al. 2005, 2009). The floral shift took place very rapidly, between latest Paleocene samples ~8 m below the onset of the CIE and PETM samples 2–3 m above the onset (Wing et al. 2009). This implies extirpation of resident floodplain plants and expansion of the ranges of “excursion” taxa into the Bighorn Basin in <30 ka. Range expansions on the order of 1000 km are probable for some PETM immigrants (Wing et al. 2005). Megafloras from the middle of the PETM (60–80 ka post onset of the CIE) show continued dominance by Fabaceae and other families with modern relatives in dry tropical forest, but during the recovery phase of the CIE, many typical late Paleocene–early Eocene plants returned (Wing et al. 2009). Late or post-CIE floras were once again dominated by long-ranging Paleocene-Eocene plants, accompanied by a few diagnostic Eocene forms that were intercontinental immigrants from Europe or Asia (Wing et al. 2005, 2009). The appearance in late or post-PETM time of taxa from other continents is also documented in palynofloras of the adjacent Powder River Basin (Wing et al. 2003).

Although the PETM had a dramatic effect on megafloreal composition, palynofloral change in the same sections is subtle, with the bald cypress, birch, and walnut families abundant throughout the Paleocene-Eocene interval (Harrington 2001; Wing et al. 2003, 2005). PETM palynofloras differ from those immediately before and after only in rare occurrences of pollen types from the Gulf Coastal plain, which otherwise do not occur so far north (Wing et al. 2005). The continued abundance of long-ranging pollen types during the PETM may reflect low pollen production by the immigrants and high pollen production by the small remaining populations of Paleocene taxa (Wing et al. 2005).

In other parts of the world, PETM floral change is known exclusively from pollen assemblages. Palynofloras cored from Lomonosov Ridge in the Arctic Ocean show decreased abundance of conifers and increased abundance of angiosperms during the PETM (Sluijs et al. 2006), a pattern also seen in biomarkers (Schouten et al. 2007). The Kumara-2 core from New Zealand shows

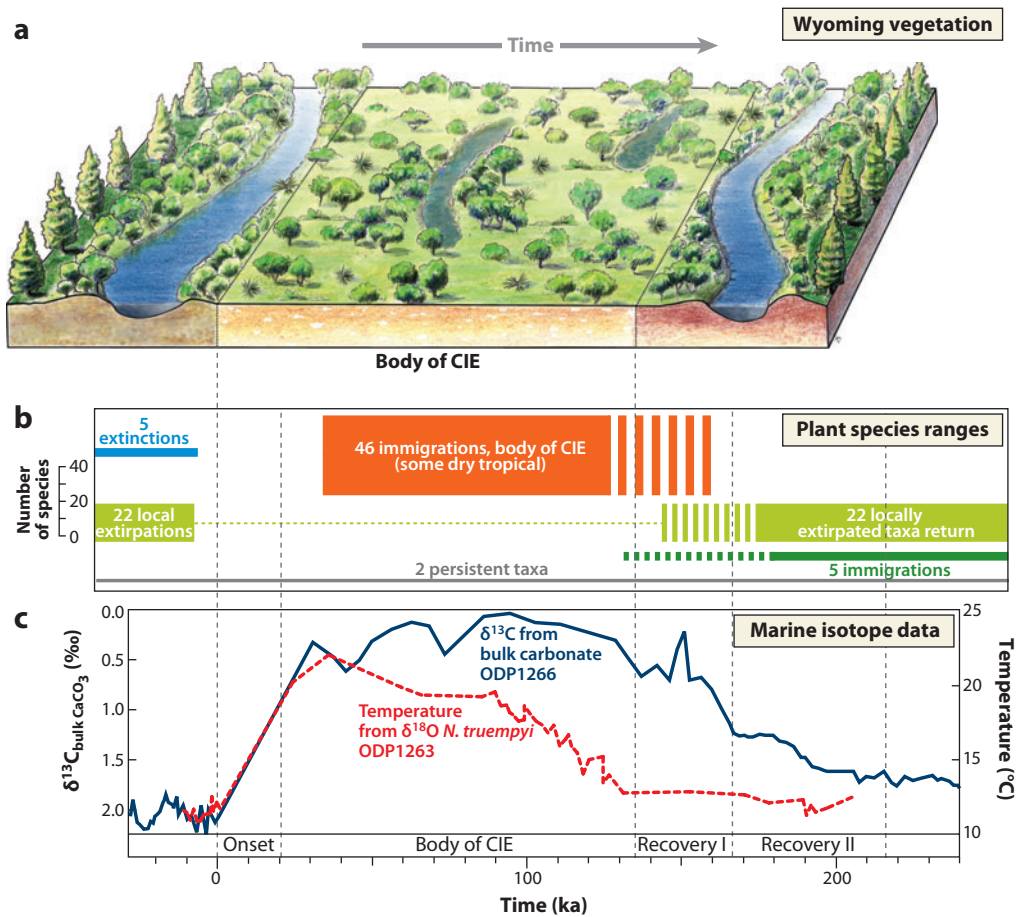


Figure 4

Vegetation change and floral turnover through the Paleocene–Eocene Thermal Maximum (PETM) in the Bighorn Basin, Wyoming. (a) During the body of the carbon isotopic excursion (CIE), vegetation was probably more open because of water stress caused by seasonal precipitation and higher evapotranspiration related to warmer temperature. Conifers were absent during the body of the CIE but present immediately before the onset and during the recovery phase. Drawing by Zell Stoltzfus. (b) Diagram showing types of plant species ranges: blue, 5 Paleocene taxa that went extinct near the onset of the CIE; light green, 22 taxa, many related to living temperate plants, that were not found during the body of the CIE but were present before and after (e.g., the conifer *Metasequoia*); orange, 46 taxa that in Wyoming are known only from the CIE (some related to living dry tropical plants); dark green, 5 Eocene immigrants, most related to living temperate plants; gray, 2 types of plant that occur throughout: leaves of the palm *Sabalites* and winged fruits of *Deviaucer*. (c) Bulk carbonate carbon isotope record from Ocean Drilling Program Site 1266 on Walvis Ridge and timescale from Murphy et al. (2010). Oxygen isotope ratio of benthic foraminifera (*N. truempyi*) from Ocean Drilling Program Site 1263 (McCarren et al. 2008) is on timescale of Murphy et al. (2010). Correlation to the Bighorn Basin is from Wing et al. (2005).

mostly stable plant communities across the PETM with modest changes that include first occurrences of the tropical mangrove palm, *Nyssa*, and a warm-climate eudicot *Cupaneidites* (Crouch et al. 2009). Palynofloras from northern South America increase in diversity through the late Paleocene–early Eocene because of diversification within many groups already present in the region during the late Paleocene (Jaramillo 2002, Jaramillo et al. 2006). Recently it has been shown that this diversity increase begins during the PETM, suggesting that tropical plants were not adversely affected by rising temperatures (Jaramillo et al. 2010).

Harrington & Jaramillo (2007) noted declining terrestrial palynomorph diversity across the Paleocene-Eocene boundary in the Gulf Coastal Plain of Mississippi, and they suggested the possibility of elevated extinction among paratropical plants during the PETM. Recent work by van Rooij (2009), however, suggests a lower stratigraphic position for the CIE. Therefore, the 35% decrease in palynomorph diversity could represent the early Eocene cool interval also seen in Rocky Mountain floras (Wing et al. 2000) rather than warming during the PETM.

Only one study has directly examined the effect of the PETM on trophic interactions among terrestrial organisms. Currano et al. (2008) found that fossil leaves from the PETM had suffered significantly higher rates of insect damage than those in late Paleocene and post-PETM-early Eocene. They also found that specialized types of insect feeding were more common. This increase could have been caused by higher temperature (increasing insect populations and metabolic rates), higher CO₂ (leading to decreased protein in leaves and higher feeding rates), or both (Currano et al. 2008).

DISCUSSION

Scientists have been aware of the PETM for two decades, and the event has been the topic of hundreds of research papers, multiple conferences and symposia, scores of news reports, and thousands of Internet postings. What have we learned from the PETM about connections between the carbon cycle, climate, and biosphere, and how well has it held up as a model for future anthropogenic global warming?

Research on the PETM has resoundingly confirmed several basic ideas about the Earth system. A release of thousands of petagrams of carbon (an amount comparable to that likely to be released by human activities) did, as expected, cause global warming and deep-ocean acidification (IPCC 2007). The climatic perturbations from the PETM persisted for ~200 ka, as anticipated for climate change driven by fossil fuel emission (Archer et al. 2009). Also as predicted, the changing climatic and oceanographic conditions drove rapid adjustments in the geographic ranges of most forms of life, regardless of habitat, trophic level, or prior distribution.

There are also some fundamental unresolved questions in PETM research, including how much carbon was released from which source(s). After initial wide acceptance of a methane clathrate source, significant objections have emerged. As detailed above the highly depleted carbon isotope composition of clathrates makes it difficult to satisfy the requirements of carbonate dissolution, warming, and the CIE. Furthermore, the Paleocene clathrate reservoir may have been too small to produce the CIE (Buffett & Archer 2004). Future research into *p*CO₂ changes across the PETM will better constrain climate sensitivity and help evaluate the potential sources of carbon. The release of carbon from Antarctic permafrost and peat can explain the observed carbonate dissolution, warming, and CIE and also provides a cohesive explanation for the magnitude and pacing of the PETM and subsequent hyperthermals (DeConto et al. 2010). In addition, the rapid recovery of the CIE suggests the role of the biosphere and soil carbon in carbon sequestration (Bowen & Zachos 2010). These processes have implications for understanding the potential climate impacts of permafrost thawing and biospheric carbon sequestration in modern climate change (IPCC 2007).

Although interest in the PETM is in large part stimulated and funded because of its parallels with anthropogenic global warming, differences between the two have come into sharper focus in recent years. The carbon release that caused the carbon isotope excursion at the PETM probably took at least 8 ka, roughly 15 times longer than any anticipated anthropogenic carbon release. This much slower rate of carbon addition translates to much less severe acidification and carbonate

dissolution in the surface ocean, presumably with less severe consequences for surface-dwelling organisms during the PETM than in the coming centuries (Ridgwell & Schmidt 2010).

Some aspects of the biotic response to the PETM are predictable, whereas others are surprising. Many of the biotic effects of the PETM appear to have been driven by increasing temperature, with no clear effects yet demonstrated from changes in ocean chemistry or atmospheric $p\text{CO}_2$. It is surprising that cool-adapted species already living at higher latitudes before the onset of the PETM are not known to have experienced major extinctions. Do low extinction levels at the PETM (except for benthic forams) reflect the existence of cool refugia or the ability of high-latitude taxa to adapt to warmer climate during the PETM? Another unexpected pattern is that the highest levels of extinction are observed in benthic forams—a group that is highly dispersable and tends to have large geographic ranges (Thomas 2007). High extinction levels suggest that changes in deep benthic environments left few refugia for benthic forams, but relatively low extinction in other deep-sea taxa point to conditions that were particularly harsh for benthic forams.

This absence of significant extinction in most groups is particularly interesting in light of the predictions of substantial future extinction with anthropogenic global warming. Projections are $\sim 35\%$ extinction globally across many groups for $>2^\circ\text{C}$ of warming (Thomas et al. 2004). The higher rate of environmental change in future projections does not explain the higher extinction rates in the models, because Thomas et al. (2004) effectively assumed instantaneous dispersal. Projected future rates of extinction may be higher than observed fossil rates because the projections include species with small geographic ranges (narrow climatic tolerances) that are unlikely to be detected in the fossil record at all. It is also possible that the ability of species to exist outside their current climatic envelopes has been underestimated. Low levels of extinction in the face of rapid environmental change during the Quaternary pose a similar challenge to modeled extinctions under future greenhouse warming (Botkin et al. 2007).

Rapid evolution is an expected consequence of rapid environmental change (Davis et al. 2005), and though the selective factors that caused rapid evolution during the PETM are not well understood, dwarfing was common in terrestrial vertebrates (Chester et al. 2010; Gingerich 1989, 2003), soil-living invertebrates (Smith et al. 2009), and some forams (Kaiho et al. 2006). In both marine and terrestrial realms, declining productivity/food availability is a potential cause of evolution to smaller body size (Chester et al. 2010, Kaiho et al. 2006). Even the evolution of larger size in some planktic forams may relate to lower productivity of surface waters in the open ocean and the need for algal symbiotes (Kaiho et al. 2006). If there is a generalization to be made about what forces evolutionary change during the PETM it would seem to be this: A warmer world is a hungrier world.

SUMMARY POINTS

1. The Paleocene-Eocene Thermal Maximum, which took place ~ 56 Mya and lasted for ~ 200 ka, stands as the most dramatic geological confirmation of greenhouse theory—increased CO_2 in the atmosphere warmed Earth's surface.
2. The large release of organic, ^{13}C -depleted carbon caused a global carbon isotopic excursion, widespread deep-ocean acidification, and carbonate dissolution.
3. Carbon was removed from the exogenic pool on a timescale of ~ 100 ka, primarily through silicate weathering and eventual precipitation of carbonate in the ocean and/or uptake by the biosphere and subsequent burial as organic carbon.

4. Warming associated with the carbon release implies approximately two doublings of atmospheric $p\text{CO}_2$ unless climate sensitivity was significantly different during the Paleogene.
5. Although there was a major extinction of benthic foraminifera, most groups of organisms did not suffer mass extinction.
6. Geographic distributions of most kinds of organisms were radically rearranged by 5–8°C of warming, with tropical forms moving poleward in both marine and terrestrial realms.
7. Rapid morphological change occurred in both marine and terrestrial lineages, suggesting that organisms adjusted to climate change through evolution as well as dispersal and local extirpation. Where best understood, these evolutionary changes appear to be responses to nutrient and/or food limitation.
8. Research on the PETM and other intervals of rapid global change has been driven by the idea that they provide geological parallels to future anthropogenic warming, but much remains to be done to gain information that can be acted on.

DISCLOSURE STATEMENT

The authors are not aware of any affiliations, memberships, funding, or financial holdings that might be perceived as affecting the objectivity of this review.

ACKNOWLEDGMENTS

We thank our many colleagues who shared their ideas, comments, and in-press manuscripts freely. We apologize for the hundreds of papers we were aware of but could not cite. Thank you to Kate Freeman, Lee Kump, and Will Clyde for thoughtful discussions and comments on the manuscript. Thanks also to Zell Stoltzfus, who drew the reconstruction, and Brandon Murphy and Heather McCarren, who provided data for **Figure 4**.

LITERATURE CITED

- Abbot DS, Tziperman E. 2009. Controls on the activation and strength of a high-latitude convective cloud feedback. *J. Atmos. Sci.* 66:519–29
- Agnini C, Fornaciari E, Rio D, Tateo F, Backman J, Giusberti L. 2007. Responses of calcareous nannofossil assemblages, mineralogy and geochemistry to the environmental perturbations across the Paleocene/Eocene boundary in the Venetian Pre-Alps. *Mar. Micropaleontol.* 63:19–38
- Alegret L, Ortiz S, Arenillas I, Molina E. 2010. What happens when the ocean is overheated? The foraminiferal response across the Paleocene–Eocene Thermal Maximum at the Alamedilla section (Spain). *Geol. Soc. Am. Bull.* 122:1616–24
- Alegret L, Ortiz S, Molina E. 2009a. Extinction and recovery of benthic foraminifera across the Paleocene–Eocene Thermal Maximum at the Alamedilla section (Southern Spain). *Palaeogeogr. Palaeoclimatol. Palaeoecol.* 279:186–200
- Alegret L, Ortiz S, Orue-Etxebarria X, Bernaola G, Baceta JI, et al. 2009b. The Paleocene–Eocene thermal maximum: new data on microfossil turnover at the Zumaia section, Spain. *Palaios* 25:318–28
- Angori E, Bernaola G, Monechi S. 2007. Calcareous nannofossil assemblages and their response to the Paleocene–Eocene Thermal Maximum event at different latitudes: ODP Site 690 and Tethyan sections. *Geol. Soc. Am. Spec. Pap.* 424:69–85

- Archer D, Eby M, Brovkin V, Ridgwell A, Cao L, et al. 2009. Atmospheric lifetime of fossil fuel carbon dioxide. *Annu. Rev. Earth Planet. Sci.* 37:117–34
- Aref M, Youssef M. 2004. The benthonic foraminifera turnover at the Paleocene/Eocene Thermal Maximum Event (PETM) in the southwestern Nile Valley, Egypt. *Neues Jahrb. Geol. Paläontol.-Ab.* 234:261–89
- Arenillas I, Molina E, Schmitz B. 1999. Planktic foraminiferal and partial derivative C-13 isotopic changes across the Paleocene/Eocene boundary at Possagno (Italy). *Int. J. Earth Sci.* 88:352–64
- Aubry MP. 2000. Where should the Global Stratotype Section and Point (GSSP) for the Paleocene/Eocene boundary be located? *Bull. Soc. Geol. Fr.* 171:461–76
- Aubry MP, Lucas S, Berggren WA, eds. 1998. *Late Paleocene-Early Eocene Climatic and Biotic Events in the Marine and Terrestrial Records*. New York: Columbia Univ. Press
- Aziz HA, Hilgen FJ, van Luijk GM, Sluijs A, Kraus MJ, et al. 2008. Astronomical climate control on paleosol stacking patterns in the upper Paleocene-lower Eocene Willwood Formation, Bighorn Basin, Wyoming. *Geology* 36:531–34
- Bains S, Corfield RM, Norris RD. 1999. Mechanisms of climate warming at the end of the Paleocene. *Science* 285:724–27
- Bains S, Norris RD, Corfield RM, Bowen GJ, Gingerich PD, Koch PL. 2003. Marine-terrestrial linkages at the Paleocene-Eocene boundary. *Geol. Soc. Am. Spec. Pap.* 369:1–9
- Bains S, Norris RD, Corfield RM, Faul KL. 2000. Termination of global warmth at the Palaeocene/Eocene boundary through productivity feedback. *Nature* 407:171–74
- Beard KC. 2008. The oldest North American primate and mammalian biogeography during the Paleocene-Eocene Thermal Maximum. *Proc. Natl. Acad. Sci. USA* 105:3815–18
- Beerling DJ. 2000. Increased terrestrial carbon storage across the Palaeocene-Eocene boundary. *Palaeogeogr. Palaeoclimatol. Palaeoecol.* 161:395–405
- Berggren WA, Ouda K. 2003. Upper Paleocene-lower Eocene planktonic foraminiferal biostratigraphy of the Dababiya section, Upper Nile Valley (Egypt). *Micropaleontology* 49:61–92
- Bolle MP, Adatte T. 2001. Palaeocene early Eocene climatic evolution in the Tethyan realm: clay mineral evidence. *Clay Minerals* 36:249–61
- Botkin DB, Saxe H, Araújo MB, Betts R, Bradshaw RHW, et al. 2007. Forecasting the effects of global warming on biodiversity. *BioScience* 57:227–36
- Boucsein B, Stein R. 2009. Black shale formation in the late Paleocene/early Eocene Arctic Ocean and paleoenvironmental conditions: new results from a detailed organic petrological study. *Mar. Petroleum Geol.* 26:416–26
- Bourque J, Hutchison JH, Holroyd P, Bloch JI. 2008. A new kinosternoid (Testudines: Dermatemydidae) from the Paleocene-Eocene boundary of the Bighorn Basin, Wyoming, and its paleoclimatological implications. *J. Vertebr. Paleontol.* 28(3):55A
- Bowen GJ, Beerling DJ, Koch PL, Zachos JC, Quattlebaum T. 2004. A humid climate state during the Palaeocene/Eocene thermal maximum. *Nature* 432:495–99
- Bowen GJ, Bowen BB. 2008. Mechanisms of PETM global change constrained by a new record from central Utah. *Geology* 36:379–82
- Bowen GJ, Bralower TJ, Delaney ML, Dickens GR, Kelly DC, et al. 2006. Eocene hyperthermal event offers insight into greenhouse warming. *EOS Trans. Am. Geophys. Union* 87:165–69
- Bowen GJ, Clyde WC, Koch PL, Ting SY, Alroy J, et al. 2002. Mammalian dispersal at the Paleocene/Eocene boundary. *Science* 295:2062–65
- Bowen GJ, Koch PL, Gingerich PD, Norris RD, Bains S, Corfield R. 2001. Refined isotope stratigraphy across the continental Paleocene-Eocene boundary on Polecat Bench in the northern Bighorn Basin. *Univ. Mich. Pap. Paleontol.* 33:73–88
- Bowen GJ, Koch PL, Meng J, Ye J, Ting SY. 2005. Age and correlation of fossiliferous late Paleocene-early eocene strata of the Erlian basin, Inner Mongolia, China. *Am. Mus. Novit.* 3474:1–26
- Bowen GJ, Zachos JC. 2010. Rapid carbon sequestration at the termination of the Palaeocene-Eocene Thermal Maximum. *Nat. Geosci.* 3:866–69
- Bown P, Pearson P. 2009. Calcareous plankton evolution and the Paleocene/Eocene thermal maximum event: new evidence from Tanzania. *Mar. Micropaleontol.* 71:60–70

- Bralower TJ. 2002. Evidence of surface water oligotrophy during the Paleocene-Eocene thermal maximum: nannofossil assemblage data from Ocean Drilling Program Site 690, Maud Rise, Weddell Sea. *Paleoceanography* 17:1023
- Breecker DO, Sharp ZD, McFadden LD. 2010. Atmospheric CO₂ concentrations during ancient greenhouse climates were similar to those predicted for A.D. 2100. *Proc. Natl. Acad. Sci. USA* 107:576–80
- Buffett B, Archer D. 2004. Global inventory of methane clathrate: sensitivity to changes in the deep ocean. *Earth Planet. Sci. Lett.* 227:185–99
- Bujak JP, Brinkhuis H. 1998. Global warming and dinocyst changes across the Paleocene/Eocene Epoch boundary. See Aubry et al. 1998, pp. 277–95
- Cecil CB, DuLong FT. 2003. Precipitation models for sediment supply in warm climates. *Soc. Sediment. Geol. Spec. Publ.* 77:21–27
- Chester S, Bloch J, Secord R, Boyer D. 2010. A new small-bodied species of *Palaeonictis* (Creodonta, Oxyaenidae) from the Paleocene-Eocene Thermal Maximum. *J. Mamm. Evol.* 17:227–43
- Clyde WC, Gingerich PD. 1998. Mammalian community response to the Latest Paleocene Thermal Maximum: an isotaphonomic study in the northern Bighorn Basin, Wyoming. *Geology* 26:1011–14
- Clyde WC, Khan IH, Gingerich PD. 2003. Stratigraphic response and mammalian dispersal during initial India-Asia collision: evidence from the Ghazij Formation, Balochistan, Pakistan. *Geology* 31:1097–100
- Colosimo A, Bralower TJ, Zachos JC. 2006. Evidence for lysocline shoaling at the Paleocene/Eocene Thermal Maximum on Shatsky Rise, Northwest Pacific. In *Proceedings of the Ocean Drilling Program, Scientific Results*, Vol. 198, ed. TJ Bralower, IP Silva, MJ Malone, pp. 1–36. College Station, TX: Ocean Drilling Prog.
- Crouch EM, Dickens GR, Brinkhuis H, Aubry MP, Hollis CJ, et al. 2003. The *Apectodinium* acme and terrestrial discharge during the Paleocene-Eocene thermal maximum: new palynological, geochemical and calcareous nannoplankton observations at Tawanui, New Zealand. *Palaeogeogr. Palaeoclimatol. Palaeoecol.* 194:387–403
- Crouch EM, Heilmann-Clausen C, Brinkhuis H, Morgans HEG, Rogers KM, et al. 2001. Global dinoflagellate event associated with the Late Paleocene Thermal Maximum. *Geology* 29:315–18
- Crouch EM, Raine JI, Kennedy EM, Handley L, Pancost RD. 2009. New Zealand terrestrial and marginal marine records across the Paleocene-Eocene transition. *Proc. Climat. Biotic Events Paleogene (CBEP 2009)*, Wellington, N. Z., Jan. 12–15, pp. 40–43. Lower Hutt, N. Z.: Inst. Geol. Nucl. Sci.
- Curran ED, Wilf P, Wing SL, Labandeira CC, Lovelock EC, Royer DL. 2008. Sharply increased insect herbivory during the Paleocene-Eocene thermal maximum. *Proc. Natl. Acad. Sci. USA* 105:1960–64
- Davis MB, Shaw RG, Etterson JR. 2005. Evolutionary responses to changing climate. *Ecology* 86:1704–14
- DeConto R, Galeotti S, Pagani M, Tracy DM, Pollard D, Beerling DJ. 2010. *Hyperternals and orbitally paced permafrost soil organic carbon dynamics*. Presented at AGU Fall Meet., Dec. 13–17, San Francisco (Abstr. PP21E-08)
- Dickens GR. 2000. Methane oxidation during the Late Palaeocene Thermal Maximum. *Bull. Soc. Geol. Fr.* 171:37–49
- Dickens GR, Castillo MM, Walker JCG. 1997. A blast of gas in the latest Paleocene: simulating first-order effects of massive dissociation of oceanic methane hydrate. *Geology* 25:259–62
- Dickens GR, Oneil JR, Rea DK, Owen RM. 1995. Dissociation of oceanic methane hydrate as a cause of the carbon-isotope excursion at the end of the Paleocene. *Paleoceanography* 10:965–71
- Diefendorf AF, Mueller KE, Wing SL, Koch PL, Freeman KH. 2010. Global patterns in leaf ¹³C discrimination and implications for studies of past and future climate. *Proc. Natl. Acad. Sci. USA* 107:5738–43
- Egger H, Homayoun M, Huber H, Rogl F, Schmitz B. 2005. Early Eocene climatic, volcanic, and biotic events in the northwestern Tethyan Untersberg section, Austria. *Palaeogeogr. Palaeoclimatol. Palaeoecol.* 217:243–64
- Farley KA, Eltgroth SF. 2003. An alternative age model for the Paleocene-Eocene thermal maximum using extraterrestrial He-3. *Earth Planet. Sci. Lett.* 208:135–48
- Fricke HC, Clyde WC, O’Neil JR, Gingerich PD. 1998. Evidence for rapid climate change in North America during the Latest Paleocene Thermal Maximum: oxygen isotope compositions of biogenic phosphate from the Bighorn Basin (Wyoming). *Earth Planet. Sci. Lett.* 160:193–208
- Fricke HC, Wing SL. 2004. Oxygen isotope and paleobotanical estimates of temperature and $\delta^{18}\text{O}$ -latitude gradients over North America during the early Eocene. *Am. J. Sci.* 304:612–35

- Gavrilov YO, Shcherbinina EA, Oberhänsli H. 2003. Paleocene-Eocene boundary events in the northeastern Peri-Tethys. *Geol. Soc. Am. Spec. Pap.* 369:147–68
- Gibbs SJ, Bown PR, Sessa JA, Bralower TJ, Wilson PA. 2006a. Nannoplankton extinction and origination across the Paleocene-Eocene Thermal Maximum. *Science* 314:1770–73
- Gibbs SJ, Bralower TJ, Bown PR, Zachos JC, Bybell LM. 2006b. Shelf and open-ocean calcareous phytoplankton assemblages across the Paleocene-Eocene Thermal Maximum: implications for global productivity gradients. *Geology* 34:233–36
- Gibbs SJ, Stoll HM, Bown PR, Bralower TJ. 2010. Ocean acidification and surface water carbonate production across the Paleocene-Eocene thermal maximum. *Earth Planet. Sci. Lett.* 295:583–92
- Gibson TG, Bybell LM, Mason DB. 2000. Stratigraphic and climatic implications of clay mineral changes around the Paleocene/Eocene boundary of the northeastern US margin. *Sediment. Geol.* 134:65–92
- Gingerich PD. 1989. New earliest Wasatchian mammalian fauna from the Eocene of northwestern Wyoming: composition and diversity in a rarely sampled high-floodplain assemblage. *Univ. Mich. Pap. Paleontol.* 28:1–97
- Gingerich PD, ed. 2001. *Paleocene-Eocene Stratigraphy and Biotic Change in the Bighorn and Clarks Fork Basins, Wyoming*. Univ. Mich. Pap. Paleontol. Vol. 33. Ann Arbor, MI: Univ. Mich. 198 pp.
- Gingerich PD. 2003. Mammalian responses to climate change at the Paleocene-Eocene boundary: Polecat Bench record in the northern Bighorn Basin, Wyoming. *Geol. Soc. Am. Spec. Pap.* 369:463–78
- Gingerich PD. 2006. Environment and evolution through the Paleocene-Eocene thermal maximum. *Trends Ecol. Evol.* 21:246–53
- Giusberti L, Rio D, Agnini C, Backman J, Fornaciari E, et al. 2007. Mode and tempo of the Paleocene-Eocene thermal maximum in an expanded section from the Venetian pre-Alps. *Geol. Soc. Am. Bull.* 119:391–412
- Hallock P. 2000. Symbiont-bearing foraminifera: harbingers of global change? *Micropaleontology* 46(Suppl. 1):95–104
- Harrington G. 2001. Pollen assemblages and Paleocene-Eocene stratigraphy in the Bighorn and Clarks Fork Basins. *Univ. Mich. Pap. Paleontol.* 33:89–96
- Harrington GJ, Jaramillo CA. 2007. Paratropical floral extinction in the Late Palaeocene–Early Eocene. *J. Geol. Soc.* 164:323–32
- Hasegawa T, Yamamoto S, Pratt LM. 2006. Data report: stable carbon isotope fluctuation of long-chain n-alkanes from Leg 208 Hole 1263A across the Paleocene/Eocene boundary. In *Proc. ODP, Sci. Results*, Vol. 208, ed. D Kroon, JC Zachos, C Richter. College Station, TX: Ocean Drilling Prog.
- Higgins JA, Schrag DP. 2006. Beyond methane: towards a theory for the Paleocene-Eocene Thermal Maximum. *Earth Planet. Sci. Lett.* 245:523–37
- Hilting AK, Kump LR, Bralower TJ. 2008. Variations in the oceanic vertical carbon isotope gradient and their implications for the Paleocene-Eocene biological pump. *Paleoceanography* 23:PA3222
- Holroyd P, Hutchison J, Strait S. 2001. Turtle diversity and abundance through the lower Eocene Willwood Formation of the southern Bighorn Basin. *Univ. Mich. Pap. Paleontol.* 33:97–107
- Hooker JJ. 1998. Mammalian faunal change across the Paleocene-Eocene transition in Europe. See Aubry et al. 1998, pp. 428–50
- Hottinger L. 1998. Shallow benthic foraminifera at the Paleocene-Eocene boundary. *Strata* 9:61–64
- Huber M. 2008. A hotter greenhouse? *Science* 321:353–54
- Huber M, Sloan LC. 1999. Warm climate transitions: a general circulation modeling study of the Late Paleocene Thermal Maximum (~56 Ma). *J. Geophys. Res.-Atmos.* 104:16633–55
- Huber M, Sloan LC, Shellito C. 2003. Early Paleogene oceans and climate: a fully coupled modeling approach using the NCAR CCSM. *Geol. Soc. Am. Spec. Pap.* 369:25–47
- Intergov. Panel Clim. Change (IPCC). 2007. *Climate Change 2007: The Physical Science Basis. Contributions of Working Group I to the Fourth Assessment Report of the Intergovernmental Panel on Climate Change*. Washington, DC: IPCC
- Ivany LC, Sessa JA. 2010. *Effects of ocean warming and acidification during the Paleocene-Eocene Thermal Maximum on deep and shallow marine communities*. Presented at Ecol. Soc. Am. Annu. Meet., Pittsburgh, PA
- Jaramillo CA. 2002. Response of tropical vegetation to Paleogene warming. *Paleobiology* 28:222–43
- Jaramillo CA, Ochoa D, Contreras L, Pagani M, Carvajal-Ortiz H, et al. 2010. Effects of rapid global warming at the Paleocene-Eocene boundary on Neotropical vegetation. *Science* 330:957–61

- Jaramillo CA, Rueda MJ, Mora G. 2006. Cenozoic plant diversity in the Neotropics. *Science* 311:1893–96
- Jiang S, Wise SW. 2007. Abrupt turnover in calcareous-nannoplankton assemblages across the Paleocene/Eocene Thermal Maximum: implications for surface-water oligotrophy over the Kerguelen Plateau, Southern Indian Ocean. *USGS OF-2007-1047, Short Res. Pap. 024*, U.S. Geol. Surv. Natl. Acad., Washington, DC
- Kaiho K, Arinobu T, Ishiwatari R, Morgans HEG, Okada H, et al. 1996. Latest Paleocene benthic foraminiferal extinction and environmental changes at Tawanui, New Zealand. *Paleoceanography* 11:447–65
- Kaiho K, Takeda K, Petrizzo MR, Zachos JC. 2006. Anomalous shifts in tropical Pacific planktonic and benthic foraminiferal test size during the Paleocene-Eocene thermal maximum. *Palaeogeogr. Palaeoclimatol. Palaeoecol.* 237:456–64
- Katz ME, Pak DK, Dickens GR, Miller KG. 1999. The source and fate of massive carbon input during the Latest Paleocene Thermal Maximum. *Science* 286:1531–33
- Kelly DC, Bralower TJ, Zachos JC. 1998. Evolutionary consequences of the Latest Paleocene Thermal Maximum for tropical planktonic foraminifera. *Palaeogeogr. Palaeoclimatol. Palaeoecol.* 141:139–61
- Kelly DC, Bralower TJ, Zachos JC, Silva IP, Thomas E. 1996. Rapid diversification of planktonic foraminifera in the tropical Pacific (ODP Site 865) during the Late Paleocene Thermal Maximum. *Geology* 24:423–26
- Kelly DC, Nielsen T, McCarren H, Zachos JC, Röhl U. 2010. Spatiotemporal patterns of carbonate sedimentation in the South Atlantic: implications for carbon cycling during the Paleocene-Eocene Thermal Maximum. *Palaeogeogr. Palaeoclimatol. Palaeoecol.* 293:30–40
- Kelly DC, Zachos JC, Bralower TJ, Schellenberg SA. 2005. Enhanced terrestrial weathering/runoff and surface ocean carbonate production during the recovery stages of the Paleocene-Eocene Thermal Maximum. *Paleoceanography* 20:PA4023
- Kennett JP, Stott LD. 1991. Abrupt deep-sea warming, palaeoceanographic changes and benthic extinctions at the end of the Paleocene. *Nature* 353:225–29
- Killops S, Killops V. 2005. *Introduction to Organic Geochemistry*. Malden, MA: Blackwell Sci. 2nd ed.
- Koch PL, Clyde WC, Hepple RP, Fogel ML, Wing SL, Zachos JC. 2003. Carbon and oxygen isotope records from Paleosols spanning the Paleocene-Eocene boundary, Bighorn Basin, Wyoming. *Geol. Soc. Am. Spec. Pap.* 369:49–64
- Koch PL, Zachos JC, Dettman DL. 1995. Stable-isotope stratigraphy and paleoclimatology of the Paleogene Bighorn Basin (Wyoming, USA). *Palaeogeogr. Palaeoclimatol. Palaeoecol.* 115:61–89
- Koch PL, Zachos JC, Gingerich PD. 1992. Correlation between isotope records in marine and continental carbon reservoirs near the Paleocene/Eocene boundary. *Nature* 358:319–22
- Kraus MJ, Riggins S. 2007. Transient drying during the Paleocene-Eocene Thermal Maximum (PETM): analysis of paleosols in the Bighorn Basin, Wyoming. *Palaeogeogr. Palaeoclimatol. Palaeoecol.* 245:444–61
- Kump LR, Arthur MA. 1999. Interpreting carbon-isotope excursions: carbonates and organic matter. *Chem. Geol.* 161:181–98
- Kurtz AC, Kump LR, Arthur MA, Zachos JC, Paytan A. 2003. Early Cenozoic decoupling of the global carbon and sulfur cycles. *Paleoceanography* 18:1090
- Kvenvolden KA. 1993. Gas hydrates—geological perspective and global change. *Rev. Geophys.* 31:173–87
- Lu GY, Keller G. 1995. Planktic foraminiferal faunal turnovers in the subtropical Pacific during the Late Paleocene to Early Eocene. *J. Foraminifer. Res.* 25:97–116
- Luterbacher H, Hardenbol J, Schmitz B. 2000. Decision of the voting members of the International Subcommission on Paleogene Stratigraphy on the criterion for the recognition of the Paleocene/Eocene boundary. *Newsl. Int. Subcomm. Paleogene Stratigr.* 9:13
- Magioncalda R, Dupuis C, Smith T, Steurbaut E, Gingerich PD. 2004. Paleocene-Eocene carbon isotope excursion in organic carbon and pedogenic carbonate: direct comparison in a continental stratigraphic section. *Geology* 32:553–56
- McCarren H, Thomas E, Hasegawa T, Rohl U, Zachos JC. 2008. Depth dependency of the Paleocene-Eocene carbon isotope excursion: paired benthic and terrestrial biomarker records (Ocean Drilling Program Leg 208, Walvis Ridge). *Geochem. Geophys. Geosyst.* 9:Q10008
- Monechi S, Angori E, von Salis K. 2000. Calcareous nannofossil turnover around the Paleocene/Eocene transition at Alamedilla (southern Spain). *Bull. Soc. Geol. Fr.* 171:477–89

- Moore EA, Kurtz AC. 2008. Black carbon in Paleocene-Eocene boundary sediments: a test of biomass combustion as the PETM trigger. *Palaeogeogr. Palaeoclimatol. Palaeoecol.* 267:147–52
- Morsi AM, Speijer RP, Stassen P, Steurbaut E. 2011. Shallow marine ostracode turnover in response to environmental change during the Paleocene-Eocene thermal maximum in northwest Tunisia. *J. Afr. Earth Sci.* 59:243–68
- Murphy BH, Farley KA, Zachos JC. 2010. An extraterrestrial ^3He -based timescale for the Paleocene-Eocene Thermal Maximum (PETM) from Walvis Ridge, IODP Site 1266. *Geochim. Cosmochim. Acta* 74:5098–108
- Mutterlose J, Linnert C, Norris R. 2007. Calcareous nannofossils from the Paleocene-Eocene thermal maximum of the equatorial Atlantic (ODP Site 1260B): evidence for tropical warming. *Mar. Micropaleontol.* 65:13–31
- Pagani M, Caldeira K, Archer D, Zachos JC. 2006a. An ancient carbon mystery. *Science* 314:1556–57
- Pagani M, Pedentchouk N, Huber M, Sluijs A, Schouten S, et al. 2006b. Arctic hydrology during global warming at the Palaeocene/Eocene Thermal Maximum. *Nature* 442:671–75
- Panchuk K, Ridgwell A, Kump LR. 2008. Sedimentary response to Paleocene-Eocene Thermal Maximum carbon release: a model-data comparison. *Geology* 36:315–18
- Pardo A, Keller G, Oberhänsli H. 1999. Paleoecologic and paleoceanographic evolution of the Tethyan Realm during the Paleocene-Eocene transition. *J. Foraminifer. Res.* 29:37–57
- Pearson PN, Palmer MR. 2000. Atmospheric carbon dioxide concentrations over the past 60 million years. *Nature* 406:695–99
- Petrizzo MR. 2007. The onset of the Paleocene-Eocene Thermal Maximum (PETM) at Sites 1209 and 1210 (Shatsky Rise, Pacific Ocean) as recorded by planktonic foraminifera. *Mar. Micropaleontol.* 63:187–200
- Pujalte V, Schmitz B, Baceta JI, Orue-Etxebarria X, Bernaola G, et al. 2009. Correlation of the Thanetian-Ilerdian turnover of larger foraminifera and the Paleocene-Eocene Thermal Maximum: confirming evidence from the Campo area (Pyrenees, Spain). *Geol. Acta* 7:161–75
- Rad S, Basile-Doelsch I, Quesnel F, Dupuis C. 2009. Silicium isotopes as a proxy of weathering processes during the PETM. *Geochim. Cosmochim. Acta* 73:A1066 (Abstr.)
- Raffi I, Backman J, Palike H. 2005. Changes in calcareous nannofossil assemblages across the Paleocene/Eocene transition from the paleo-equatorial Pacific Ocean. *Palaeogeogr. Palaeoclimatol. Palaeoecol.* 226:93–126
- Raffi I, Backman J, Zachos JC, Sluijs A. 2009. The response of calcareous nannofossil assemblages to the Paleocene Eocene Thermal Maximum at the Walvis Ridge in the South Atlantic. *Mar. Micropaleontol.* 70:201–12
- Ravizza G, Norris RN, Blusztajn J, Aubry MP. 2001. An osmium isotope excursion associated with the Late Paleocene Thermal Maximum: evidence of intensified chemical weathering. *Paleoceanography* 16:155–63
- Ridgwell A. 2007. Interpreting transient carbonate compensation depth changes by marine sediment core modeling. *Paleoceanography* 22:PA4102
- Ridgwell A, Schmidt DN. 2010. Past constraints on the vulnerability of marine calcifiers to massive CO_2 release. *Nat. Geosci.* 3:196–200
- Robert C, Kennett JP. 1994. Antarctic subtropical humid episode at the Paleocene-Eocene boundary—clay-mineral evidence. *Geology* 22:211–14
- Röhl U, Norris RD, Ogg JG. 2003. Cyclostratigraphy of upper Paleocene and lower Eocene sediments at Blake Nose Site 1051 (western North Atlantic). *Geol. Soc. Am. Spec. Pap.* 369:567–88
- Röhl U, Westerhold T, Bralower TJ, Zachos JC. 2007. On the duration of the Paleocene-Eocene Thermal Maximum (PETM). *Geochim. Geophys. Geosyst.* 8:Q12002
- Rose KD. 1981. *The Clarkforkian Land-Mammal Age and Mammalian Faunal Composition Across the Paleocene-Eocene Boundary*. Univ. Mich. Pap. Paleontol. Vol. 26. Ann Arbor, MI: Univ. Mich. 197 pp.
- Royer DL. 2006. CO_2 -forced climate thresholds during the Phanerozoic. *Geochim. Cosmochim. Acta* 70:5665–75
- Royer DL, Wing SL, Beerling DJ, Jolley DW, Koch PL, et al. 2001. Paleobotanical evidence for near present-day levels of atmospheric CO_2 during part of the tertiary. *Science* 292:2310–13
- Scheibner C, Speijer R. 2008. Decline of coral reefs during late Paleocene to early Eocene global warming. *eEarth* 3:19–26
- Scheibner C, Speijer RP, Marzouk AM. 2005. Turnover of larger foraminifera during the Paleocene-Eocene Thermal Maximum and paleoclimatic control on the evolution of platform ecosystems. *Geology* 33:493–96

- Schmitz B, Pujalte V. 2007. Abrupt increase in seasonal extreme precipitation at the Paleocene-Eocene boundary. *Geology* 35:215–18
- Schmitz B, Pujalte V, Nunez-Betelu K. 2001. Climate and sea-level perturbations during the initial eocene thermal maximum: evidence from siliciclastic units in the Basque Basin (Ermua, Zumaia and Trabakua Pass), northern Spain. *Palaeoogeogr. Palaoclimatol. Palaeoecol.* 165:299–320
- Schouten S, Woltering M, Rijpstra WIC, Sluijs A, Brinkhuis H, Damste JSS. 2007. The Paleocene-Eocene carbon isotope excursion in higher plant organic matter: differential fractionation of angiosperms and conifers in the Arctic. *Earth Planet. Sci. Lett.* 258:581–92
- Scotese CR. 2010. *The PALEOMAP Project PaleoAtlas for ArcGIS*, Vol. 1: *Cenozoic Paleogeographic and Plate Tectonic Reconstructions*. Arlington, Tex.: PALEOMAP Project
- Secord R, Chester S, Bloch J, Boyer D, Krigbaum J. 2008. The first North American equids: a high-resolution stratigraphic study in the Paleocene-Eocene Thermal Maximum. *J. Vertebr. Paleontol.* 28:140A
- Secord R, Gingerich PD, Lohmann KC, MacLeod KG. 2010. Continental warming preceding the Palaeocene-Eocene Thermal Maximum. *Nature* 467:955–58
- Secord R, Gingerich PD, Smith ME, Clyde WC, Wilf P, Singer BS. 2006. Geochronology and mammalian biostratigraphy of middle and upper Paleocene continental strata, Bighorn Basin, Wyoming. *Am. J. Sci.* 306:211–45
- Sheldon ND, Tabor NJ. 2009. Quantitative paleoenvironmental and paleoclimatic reconstruction using paleosols. *Earth-Sci. Rev.* 95:1–52
- Shellito CJ, Sloan LC. 2006. Reconstructing a lost Eocene paradise: part I. Simulating the change in global floral distribution at the initial Eocene thermal maximum. *Global Planet. Change* 50:1–17
- Sloan LC, Walker JCG, Moore TC, Rea DK, Zachos JC. 1992. Possible methane-induced polar warming in the Early Eocene. *Nature* 357:320–22
- Sluijs A, Bowen G, Brinkhuis H, Lourens L, Thomas E. 2007a. The Palaeocene-Eocene Thermal Maximum super greenhouse: biotic and geochemical signatures, age models and mechanisms of global change. In *Deep-Time Perspectives on Climate Change: Marrying the Signal from Computer Models and Biological Proxies*, ed. M Williams, AM Haywood, FJ Gregory, DN Schmidt, pp. 323–49. London: Geol. Soc.
- Sluijs A, Brinkhuis H, Schouten S, Bohaty SM, John CM, et al. 2007b. Environmental precursors to rapid light carbon injection at the Palaeocene/Eocene boundary. *Nature* 450:1218–21
- Sluijs A, Pross J, Brinkhuis H. 2005. From greenhouse to icehouse; organic-walled dinoflagellate cysts as paleoenvironmental indicators in the Paleogene. *Earth-Sci. Rev.* 68:281–315
- Sluijs A, Schouten S, Pagani M, Woltering M, Brinkhuis H, et al. 2006. Subtropical Arctic Ocean temperatures during the Palaeocene/Eocene Thermal Maximum. *Nature* 441:610–13
- Smith FA, Wing SL, Freeman KH. 2007. Magnitude of the carbon isotope excursion at the Paleocene-Eocene Thermal Maximum: the role of plant community change. *Earth Planet. Sci. Lett.* 262:50–65
- Smith JJ, Hasiotis ST, Kraus MJ, Woody DT. 2008a. Relationship of floodplain ichnocoenoses to paleopedology, paleohydrology, and paleoclimate in the Willwood Formation, Wyoming, during the Paleocene-Eocene Thermal Maximum. *Palaios* 23:683–99
- Smith JJ, Hasiotis ST, Kraus MJ, Woody DT. 2009. Transient dwarfism of soil fauna during the Paleocene-Eocene Thermal Maximum. *Proc. Natl. Acad. Sci. USA* 106:17655–60
- Smith JJ, Hasiotis ST, Woody DT, Kraus MJ. 2008b. Paleoclimatic implications of crayfish-mediated prismatic structures in paleosols of the Paleogene Willwood Formation, Bighorn Basin, Wyoming, USA. *J. Sediment. Res.* 78:323–34
- Smith KT. 2009. A new lizard assemblage from the earliest Eocene (Zone Wa0) of the Bighorn Basin, Wyoming, USA: biogeography during the warmest interval of the Cenozoic. *J. Syst. Palaeontol.* 7:299–358
- Smith T, Rose KD, Gingerich PD. 2006. Rapid Asia-Europe-North America geographic dispersal of earliest Eocene primate *Teilhardina* during the Paleocene-Eocene Thermal Maximum. *Proc. Natl. Acad. Sci. USA* 103:11223–27
- Speijer RP, Morsi AMM. 2002. Ostracode turnover and sea-level changes associated with the Paleocene-Eocene Thermal Maximum. *Geology* 30:23–26
- Steineck PL, Thomas E. 1996. The latest Paleocene crisis in the deep sea: Ostracode succession at Maud Rise, Southern Ocean. *Geology* 24:583–86

- Strait SG. 2001. New Wa0 mammalian fauna from Castle Gardens in the southeastern Bighorn Basin. *Univ. Mich. Pap. Paleontol.* 33:127–43
- Svensen H, Planke S, Corfu F. 2010. Zircon dating ties NE Atlantic sill emplacement to initial Eocene global warming. *J. Geol. Soc.* 167:433–36
- Svensen H, Planke S, Malthe-Sorensen A, Jamtveit B, Myklebust R, et al. 2004. Release of methane from a volcanic basin as a mechanism for initial Eocene global warming. *Nature* 429:542–45
- Thiry M, Dupuis M. 2000. Use of clay minerals for paleoclimatic reconstructions: limits of the method with special reference to the Paleocene–lower Eocene interval. *GFF* 122:166–67
- Thomas CD, Cameron A, Green RE, Bakkenes M, Beaumont LJ, et al. 2004. Extinction risk from climate change. *Nature* 427:145–48
- Thomas DJ, Zachos JC, Bralower TJ, Thomas E, Bohaty S. 2002. Warming the fuel for the fire: evidence for the thermal dissociation of methane hydrate during the Paleocene-Eocene Thermal Maximum. *Geology* 30:1067–70
- Thomas E. 1989. Development of Cenozoic deep-sea benthic foraminiferal faunas in Antarctic waters. *Geol. Soc. Lond. Spec. Publ.* 47:283–96
- Thomas E. 1998. Biogeography of the late Paleocene benthic foraminiferal extinction. See Aubry et al. 1998, pp. 214–43
- Thomas E. 2003. Extinction and food at the seafloor: A high-resolution benthic foraminiferal record across the initial Eocene Thermal Maximum, Southern Ocean Site 690. *Geol. Soc. Am. Spec. Pap.* 369:319–32
- Thomas E. 2007. Cenozoic mass extinctions in the deep sea: What perturbs the largest habitat on Earth? *Geol. Soc. Am. Spec. Pap.* 424:1–23
- Thomas E, Shackleton NJ. 1996. The Paleocene-Eocene benthic foraminiferal extinction and stable isotope anomalies. In *Correlation of the Early Paleogene in Northwest Europe Correlation of the Early Paleogene in Northwest Europe*, Spec. Pub. 101, ed. RWOB Knox, R Corfield, RE Dunay, pp. 401–41. Washington, DC: Geol. Soc.
- Tjalsma R, Lohmann G. 1983. *Paleocene-Eocene Bathyal and Abyssal Benthic Foraminifera from the Atlantic Ocean*. Washington, DC: Micropaleontol. Press/American Museum of Natural History.
- Torfstein A, Winckler G, Tripati A. 2010. Productivity feedback did not terminate the Paleocene-Eocene Thermal Maximum (PETM). *Clim. Past Discuss.* 5:2391–410
- Tremolada F, Bralower TJ. 2004. Nannofossil assemblage fluctuations during the Paleocene-Eocene Thermal Maximum at Sites 213 (Indian Ocean) and 401 (North Atlantic Ocean): palaeoceanographic implications. *Mar. Micropaleontol.* 52:107–16
- Tripati A, Elderfield H. 2005. Deep-sea temperature and circulation changes at the Paleocene-Eocene Thermal Maximum. *Science* 308:1894–98
- van Roij L. 2009. *The Paleocene-Eocene Thermal Maximum in the Gulf of Mexico*. Utrecht, The Netherlands: Department of Earth Sciences, Faculty of Geosciences, Utrecht University.
- Villasante-Marcos V, Hollis CJ, Dickens GR, Nicolo MJ. 2009. Rock magnetic properties across the Paleocene-Eocene Thermal Maximum in Marlborough, New Zealand. *Geol. Acta* 7:229–42
- Webb AE, Leighton LR, Schellenberg SA, Landau EA, Thomas E. 2009. Impact of the Paleocene-Eocene Thermal Maximum on deep-ocean microbenthic community structure: using rank-abundance curves to quantify paleoecological response. *Geology* 37:783–86
- Weijers JWH, Schouten S, Sluijs A, Brinkhuis H, Damste JSS. 2007. Warm Arctic continents during the Paleocene-Eocene Thermal Maximum. *Earth Planet. Sci. Lett.* 261:230–38
- Westerhold T, Rohl U, McCarren HK, Zachos JC. 2009. Latest on the absolute age of the Paleocene-Eocene Thermal Maximum (PETM): new insights from exact stratigraphic position of key ash layers +19 and –17. *Earth Planet. Sci. Lett.* 287:412–19
- Wing SL. 1998. Late Paleocene-Early Eocene floral and climatic change in the Bighorn Basin, Wyoming. See Aubry et al. 1998, pp. 380–400
- Wing SL, Alroy J, Hickey LJ. 1995. Plant and mammal diversity in the Paleocene to early Eocene of the Bighorn Basin. *Palaeogeogr. Palaeoclimatol. Palaeoecol.* 115:117–55
- Wing SL, Bao H, Koch PL. 2000. An early Eocene cool period? Evidence for continental cooling during the warmest part of the Cenozoic. In *Warm Climates in Earth History*, ed. BT Huber, KG MacLeod, SL Wing, pp. 197–237. Cambridge: Cambridge University Press

- Wing SL, Bloch JI, Bowen GJ, Boyer DM, Chester S, et al. 2009. Coordinated sedimentary and biotic change during the Paleocene-Eocene Thermal Maximum in the Bighorn Basin, Wyoming, USA. *Proc. Climat. Biotic Events Paleogene (CBEP 2009)*, Wellington, N. Z., Jan. 12–15, pp. 157–63. Lower Hutt, N. Z.: Inst. Geol. Nucl. Sci.
- Wing SL, Harrington GJ. 2001. Floral response to rapid warming in the earliest Eocene and implications for concurrent faunal change. *Paleobiology* 27:539–63
- Wing SL, Harrington GJ, Bowen GJ, Koch PL. 2003. Floral change during the Initial Eocene Thermal Maximum in the Powder River Basin, Wyoming. *Geol. Soc. Am. Spec. Pap.* 369:425–40
- Wing SL, Harrington GJ, Smith FA, Bloch JI, Boyer DM, Freeman KH. 2005. Transient floral change and rapid global warming at the Paleocene-Eocene boundary. *Science* 310:993–96
- Winguth A, Shellito C, Shields C, Winguth C. 2010. Climate response at the Paleocene-Eocene Thermal Maximum to greenhouse gas forcing—a model study with CCSM3. *J. Clim.* 23:2562–84
- Wynn JG. 2007. Carbon isotope fractionation during decomposition of organic matter in soils and paleosols: implications for paleoecological interpretations of paleosols. *Palaeogeogr. Palaeoclimatol. Palaeoecol.* 251:437–48
- Yom-Tov Y, Geffen E. 2006. Geographic variation in body size: the effects of ambient temperature and precipitation. *Oecologia* 148:213–18
- Zachos J, Pagani M, Sloan L, Thomas E, Billups K. 2001. Trends, rhythms, and aberrations in global climate 65 Ma to present. *Science* 292:686–93
- Zachos JC, Rohl U, Schellenberg SA, Sluijs A, Hodell DA, et al. 2005. Rapid acidification of the ocean during the Paleocene-Eocene Thermal Maximum. *Science* 308:1611–15
- Zachos JC, Schouten S, Bohaty S, Quattlebaum T, Sluijs A, et al. 2006. Extreme warming of mid-latitude coastal ocean during the Paleocene-Eocene Thermal Maximum: inferences from TEX86 and isotope data. *Geology* 34:737–40
- Zachos JC, Wara MW, Bohaty S, Delaney ML, Petrizzo MR, et al. 2003. A transient rise in tropical sea surface temperature during the Paleocene-Eocene Thermal Maximum. *Science* 302:1551–54
- Zeebe RE, Zachos JC, Dickens GR. 2009. Carbon dioxide forcing alone insufficient to explain Palaeocene-Eocene Thermal Maximum warming. *Nat. Geosci.* 2:576–80



Contents

Plate Tectonics, the Wilson Cycle, and Mantle Plumes: Geodynamics from the Top <i>Kevin Burke</i>	1
Early Silicate Earth Differentiation <i>Guillaume Caro</i>	31
Building and Destroying Continental Mantle <i>Cin-Ty A. Lee, Peter Luffi, and Emily J. Chin</i>	59
Deep Mantle Seismic Modeling and Imaging <i>Thorne Lay and Edward J. Garnero</i>	91
Using Time-of-Flight Secondary Ion Mass Spectrometry to Study Biomarkers <i>Volker Thiel and Peter Sjövall</i>	125
Hydrogeology and Mechanics of Subduction Zone Forearcs: Fluid Flow and Pore Pressure <i>Demian M. Saffer and Harold J. Tobin</i>	157
Soft Tissue Preservation in Terrestrial Mesozoic Vertebrates <i>Mary Higby Schweitzer</i>	187
The Multiple Origins of Complex Multicellularity <i>Andrew H. Knoll</i>	217
Paleoecologic Megatrends in Marine Metazoa <i>Andrew M. Bush and Richard K. Bambach</i>	241
Slow Earthquakes and Nonvolcanic Tremor <i>Gregory C. Beroza and Satoshi Ide</i>	271
Archean Microbial Mat Communities <i>Michael M. Tice, Daniel C.O. Thornton, Michael C. Pope, Thomas D. Olszewski, and Jian Gong</i>	297
Uranium Series Accessory Crystal Dating of Magmatic Processes <i>Axel K. Schmitt</i>	321

A Perspective from Extinct Radionuclides on a Young Stellar Object: The Sun and Its Accretion Disk <i>Nicolas Dauphas and Marc Chaussidon</i>	351
Learning to Read the Chemistry of Regolith to Understand the Critical Zone <i>Susan L. Brantley and Marina Lebedeva</i>	387
Climate of the Neoproterozoic <i>R.T. Pierrehumbert, D.S. Abbot, A. Voigt, and D. Koll</i>	417
Optically Stimulated Luminescence Dating of Sediments over the Past 200,000 Years <i>Edward J. Rhodes</i>	461
The Paleocene-Eocene Thermal Maximum: A Perturbation of Carbon Cycle, Climate, and Biosphere with Implications for the Future <i>Francesca A. McInerney and Scott L. Wing</i>	489
Evolution of Grasses and Grassland Ecosystems <i>Caroline A.E. Strömberg</i>	517
Rates and Mechanisms of Mineral Carbonation in Peridotite: Natural Processes and Recipes for Enhanced, in situ CO ₂ Capture and Storage <i>Peter B. Kelemen, Juerg Matter, Elisabeth E. Streit, John F. Rudge, William B. Curry, and Jerzy Blusztajn</i>	545
Ice Age Earth Rotation <i>Jerry X. Mitrovica and John Wahr</i>	577
Biogeochemistry of Microbial Coal-Bed Methane <i>Dariusz Strapoć, Maria Mastalerz, Katherine Dawson, Jennifer Macalady, Amy V. Callaghan, Boris Wawrik, Courtney Turich, and Matthew Ashby</i>	617

Indexes

Cumulative Index of Contributing Authors, Volumes 29–39	657
Cumulative Index of Chapter Titles, Volumes 29–39	661

Errata

An online log of corrections to *Annual Review of Earth and Planetary Sciences* articles may be found at <http://earth.annualreviews.org>